DEPARTMENT OF ELECTRICAL AND COMPUTER ENGINEERING
COLLEGE OF ENGINEERING AND TECHNOLOGY
OLD DOMINION UNIVERSITY
NORFOLK, VA 23529

FUEL-OPTIMAL TRAJECTORIES OF AEROASSISTED ORBITAL TRANSFER WITH PLANE CHANGE

By

Desineni Subbaramaiah Naidu, Co-Principal Investigator

Joseph L. Hibey, Principal Investigator

Progress Report
For the period ended June 30, 1989

Prepared for the
National Aeronautics and Space Administration
Langley Research Center
Hampton, Virginia 23665-5225

Under
Research Grant NAG-1-736
Dr. Douglas B. Price, Technical Monitor
GCD-Spacecraft Control Branch

June 1989

DEPARTMENT OF ELECTRICAL AND COMPUTER ENGINEERING
COLLEGE OF ENGINEERING AND TECHNOLOGY
OLD DOMINION UNIVERSITY
NORFOLK, VA 23529

FUEL-OPTIMAL TRAJECTORIES OF AEROASSISTED ORBITAL TRANSFER WITH PLANE CHANGE

By

Desineni Subbaramaiah Naidu, Co-Principal Investigator

Joseph L. Hibey, Principal Investigator

Progress Report
For the period ended June 30, 1989

Prepared for the
National Aeronautics and Space Administration
Langley Research Center
Hampton, Virginia 23665-5225

Under
Research Grant NAG-1-736
Dr. Douglas B. Price, Technical Monitor
GCD-Spacecraft Control Branch

Submitted by the
Old Dominion University Research Foundation
P.O. Box 6369
Norfolk, Virginia 23508-0369

June 1989

TABLE OF CONTENTS

LIST OF FIGURES

Abstract: The fuel-optimal control problem arising in noncoplanar orbital transfer employing aeroassist technology is addressed. The mission involves the transfer from high Earth orbit to low Earth orbit with plane change. The complete maneuver consists of a deorbit impulse to inject a vehicle from a circular orbit to elliptic orbit for the atmospheric entry, a boost impulse at the exit from the atmosphere for the vehicle to attain a desired orbital altitude and finally a reorbit impulse to circularize the path of the vehicle. In order to minimize the total fuel consumption, a performance index is chosen as the sum of the deorbit, boost, and reorbit impulses. Application of Pontryagin minimum principle leads us to a nonlinear, two-point, boundary value problem, which is solved by using a multiple shooting method.

Nomenclature

$A_1 = C_{DO} S \rho_s H_a / 2m$

$A_2 = C_{LR} S \rho_s H_a / 2m$

$b = R_a / H_a$

C_D : drag coefficient

C_{DO}: zero-lift drag coefficient

C_L : lift coefficient

C_{LR}: lift coefficient for maximum lift-to-drag ratio

D : drag force

E_m : maximum value of L/D

g : gravitational acceleration

H : altitude

$\mathcal{H}$: Hamiltonian

i : inclination

J : performance index

K : induced drag factor

L : lift force

m : vehicle mass

R : distance from Earth center to vehicle center of gravity

R_a : radius of atmospheric boundary

R_c : radius of low Earth orbit

R_d : radius of high Earth orbit

R_E : radius of Earth

S : aerodynamic reference area

t : time

V : velocity

v : normalized velocity

β : inverse atmospheric scale height

γ : flight path angle

ψ : heading angle

σ : bank angle

θ : down range angle

ϕ : cross range angle

δ : normalized density

λ : costate (Langrange) variable

μ : gravitational constant of Earth

$\eta = C_L/C_{LR}$

ρ : density

τ : normalized time

ΔV : characteristic velocity

Δv : normalized characteristic velocity

Subscripts

c : circularization or reorbit at LEO

d : deorbit at HEO

e : entry to atmosphere

f : exit from atmosphere

s : surface level

I. INTRODUCTION

The main function of the space transportation system is to deliver payloads from Earth to various locations in space. Until now, this function has been performed by various rockets, the space shuttle, and expendable upper stages using solid or liquid propellants. In particular, considering the economic benefits and reusability, an orbital transfer vehicle (OTV) is proposed for transporting payloads between low Earth orbit (LEO) and high Earth orbit (HEO). The two basic operating modes contemplated for OTV are a ground-based OTV which returns to Earth after each mission and a space-based OTV which operates out of an orbiting hanger located at the proposed Space Station.

In a typical mission, a space-based OTV, which is initially at the space station orbit (SSO), is required to transfer a payload to geosynchronous Earth orbit (GEO), pick up another payload, say a faulty satellite, and return to rendezvous with the orbiting hanger at SSO for refurbishment and redeployment of the payload. The OTV on its return journey from GEO to SSO needs to dissipate some of its orbital energy. This can be accomplished by using an entirely propulsive (Hohmann) transfer in space only or a combination of propulsive transfer in space and aeroassisted maneuver in the

atmosphere. It has been established that a significant fuel savings and hence increased payload capabilities can be achieved with propulsive and aeroassisted maneuvers instead of all-propulsive maneuvers[1]. This leads to an aeroassisted orbital transfer vehicle (AOTV), which on its return leg of the mission, dips into the Earth's atmosphere, utilizes atmospheric drag to reduce the orbital velocity and employs lift and bank angle modulations to achieve a desired orbital inclination. Basically, the AOTV performs a synergetic maneuver, employing a hybrid combination of propulsive maneuver in space and aerodynamic maneuver in the atmosphere.

It is believed that the concept of aeroassisted orbital transfer opens new mission opportunities for the space transportation system, especially with regard to the establishment of the permanent space station. Fig. 1 shows the space transportation architecture relevant to aeroassist technology. The optimization of fuel is an important aspect of orbital transfer missions.[2-7]

In this paper, we address the fuel-optimal control problem arising in noncoplanar orbital transfer employing aeroassist technology. The maneuver involves the transfer from HEO to LEO with a plane change and at the same time minimization of the fuel consumption. It is known that the change in velocity, also called the characteristic velocity, is a convenient measure of fuel consumption. For the minimum-fuel maneuver, the objective is then to minimize the total characteristic velocity for deorbit, boost, and reorbit (or circularization) for a specified change in inclination angle. Application of Pontryagin minimum principle leads us to a nonlinear, two-point, boundary value problem (TPBVP), which is solved by using a multiple shooting method.[8-10]

II. BASIC EQUATIONS

For the orbital transfer problem, the following assumptions are made. (i) The initial HEO and final LEO orbits are circular. (ii) The mission is comprised of three impulses. (iii) The vehicle is represented as a constant point mass during atmospheric pass. (iv) A Newtonian inverse square gravitational field is used. (v) Earth's rotation is neglected. (vi) The atmosphere is exponential. (vii) The vehicle has a parabolic drag polar.

The complete mission from HEO to LEO with atmospheric pass is depicted in Fig. 2. It is composed of three impulses: first, a deorbit impulse ΔV_d at HEO to inject the vehicle into a HEO-entry elliptic orbit, second, a boost impulse ΔV_b at the exit from the atmosphere for the vehicle to attain sufficient velocity to travel along an exit-LEO elliptic orbit, and finally, a circularizing impulse ΔV_c to circularize the path of the vehicle.

Consider the basic equations of motion for different phases of deorbit, aeroassist (or atmospheric flight), boost and reorbit (or circularization).

Deorbit

Initially, we assume that the spacecraft is in a circular orbit of radius R_d, well outside the Earth's atmosphere, moving with a circular velocity $V_d = \sqrt{\mu/R_d}$. Deorbit is performed by means of an impulse ΔV_d, to transfer the vehicle from the circular orbit to elliptic orbit with perigee low enough to intersect the dense part of the atmosphere [Fig. 2]. Since the elliptic velocity at D is less than the circular velocity at D, the impulse ΔV_d is executed so as to oppose the circular velocity V_d. The deorbit impulse ΔV_d causes the vehicle to enter the atmosphere of radius R_a with a velocity V_e and flight path angle γ_e. It is known that the optimal-energy loss

maneuver from the circular orbit is simply the Hohmann transfer and the impulse is parallel and opposite to the instantaneous velocity vector.

Using the principle of conservation of energy and angular momentum at the deorbit point D, and the atmospheric entry point E, we get,[11]

$$V_e^2/2 - \mu/R_a = (V_d-\Delta V_d)^2/2 - \mu/R_d \tag{1}$$

$$R_a V_e \cos(-\gamma_e) = R_d(V_d-\Delta V_d) \tag{2}$$

from which solving for ΔV_d, we get

$$\Delta V_d = \sqrt{\mu/R_d} - \sqrt{2\mu(1/R_a-1/R_d)/\left[(R_d/R_a)^2/\cos^2\gamma_e-1\right]} \tag{3}$$

It is easily seen that the minimum value of the deorbit impulse ΔV_{dm} obtained at $\gamma_e = 0$, corresponds to an ideal transfer wherein the space vehicle grazes along the atmospheric boundary. To ensure proper atmospheric entry, the deorbit impulse ΔV_d must be higher than the minimum deorbit impulse ΔV_{dm} which is given by

$$\Delta V_{dm} = \sqrt{\mu/R_d} - \sqrt{2\mu(1/R_a-1/R_d)/\left[(R_d/R_a)^2-1\right]} \tag{4}$$

Aeroassist (Atmospheric) Flight

During the aeroassist (or atmospheric) flight, the vehicle performs a three-dimensional skip maneuver and using aerodynamic lift and bank angle achieves the necessary the plane change. In this process, the vehicle decelerates due to the atmospheric drag.

The equations of motion for the vehicle during the atmospheric pass are given below (Fig. 3). The kinematic equations are,[2]

$$\frac{dR}{dt} = V\sin\gamma \tag{5a}$$

$$\frac{d\theta}{dt} = V\cos\gamma\cos\psi/R\cos\phi \tag{5b}$$

$$\frac{d\phi}{dt} = V\cos\gamma\sin\psi/R \tag{5c}$$

The force equations are

$$m\frac{dV}{dt} = -D - mg\sin\gamma \tag{5d}$$

$$mV\frac{d\gamma}{dt} = L\cos\sigma + m(V^2/R - g)\cos\gamma \tag{5e}$$

$$mV\frac{d\psi}{dt} = L\sin\sigma/\cos\gamma - (mV^2/R)\cos\gamma\cos\psi\tan\phi \tag{5f}$$

where,

$$L = C_L\rho SV^2/2; \quad D = C_D\rho SV^2/2; \quad C_D = C_{DO} + KC_L^2$$

$$g = \mu/R^2; \quad R = H + R_E; \quad \rho = \rho_s\exp(-H\beta)$$

Using the normalized variables,

$$\tau = t/\sqrt{R_a^3/\mu}\ ; \quad v = V/\sqrt{\mu/R_a} \tag{6}$$

and the dimensionless constants,

$$h = H/H_a; \quad b = R_a/H_a; \quad \delta = \rho/\rho_s = \exp(-h\beta H_a) \tag{7a}$$

$$\eta = C_L/C_{LR}; \quad C_{LR} = \sqrt{C_{DO}/K} \tag{7b}$$

in (5), we get the normalized form as

$$\frac{dh}{d\tau} = bv\sin\gamma \tag{8a}$$

$$\frac{d\theta}{d\tau} = \frac{bv\cos\gamma\cos\psi}{(b-1+h)\cos\phi} \tag{8b}$$

$$\frac{d\phi}{d\tau} = \frac{bv\cos\gamma\sin\psi}{(b-1+h)} \tag{8c}$$

$$\frac{dv}{d\tau} = -A_1 b(1+\eta^2)\delta v^2 - \frac{b^2\sin\gamma}{(b-1+h)^2} \tag{8d}$$

$$\frac{d\gamma}{d\tau} = A_2 b\eta\delta v\cos\sigma + \frac{bv\cos\gamma}{(b-1+h)} - \frac{b^2\cos\gamma}{(b-1+h)v^2} \tag{8e}$$

$$\frac{d\psi}{d\tau} = \frac{A_2 b\delta\eta v\sin\sigma}{\cos\gamma} - \frac{bv\cos\gamma\cos\psi\tan\phi}{(b-1+h)} \tag{8f}$$

where, $A_1 = C_{DO}S\rho_s H_a/2m$; $A_2 = C_{LR}S\rho_s H_a/2m$

From the above equations of motion, we see clearly that during the atmospheric maneuver, if the lift vector L is rotated about the velocity vector V through the bank angle σ, it creates a lateral force component $L\sin\sigma$ orthogonal to the vertical plane that has the effect of changing the heading angle ψ. At the end of the maneuver, the vehicle is already in vacuum and hence there is no lift. The equations (5c) and (5f) for the cross range angle ϕ, and the heading angle ψ, become[2],

$$\frac{d\phi/dt}{d\psi/dt} = -\frac{\tan\psi}{\tan\phi} \tag{9a}$$

integration of which yields,

$$\cos\phi\cos\psi = \cos i \tag{9b}$$

where, i is the orbital inclination. For small values of cross range angle ϕ,

the orbital inclination i is given by the heading angle ψ itself. Thus, the total change in the heading corresponds to the change in orbital inclination (plane change).

Boost and Reorbit

During the atmospheric flight, the vehicle performs the desired plane change and dissipates some energy due to atmospheric drag. Therefore, a second impulse is required to boost the vehicle back to orbital altitude. The vehicle exits the atmosphere at point F, with a velocity V_f and flight path angle γ_f. The additional impulse ΔV_b, required at the exit point F for boosting into an elliptic orbit with apogee radius R_c and the reorbit impulse ΔV_c required to insert the vehicle into a circular orbit at point C, are obtained by using the principle of conservation of energy and angular momentum at the exit point F, and the circularization point C. Thus, we have,[11]

$$(V_f+\Delta V_b)^2/2 - \mu/R_a = (V_c-\Delta V_c)^2/2 - \mu/R_c \qquad (10)$$

$$(V_f+\Delta V_b)R_a\cos\gamma_f = R_c(V_c-\Delta V_c) \qquad (11)$$

Solving for ΔV_b and ΔV_c from the above equations (10) and (11),

$$\Delta V_b = \sqrt{2\mu(1/R_a-1/R_c)/\left[1-(R_a/R_c)^2\cos^2\gamma_f\right]} - V_f \qquad (12)$$

$$\Delta V_c = \sqrt{\mu/R_c} - \sqrt{2\mu(1/R_a-1/R_c)/\left[(R_c/R_a)^2/\cos^2\gamma_f-1\right]} \qquad (13)$$

Finally, the vehicle is in a circular orbit (of radius R_c) moving with the velocity $V_c = \sqrt{\mu/R_c}$.

III. OPTIMAL CONTROL

For the minimum-fuel maneuver, the objective is then to minimize the total characteristic velocity for a specified change in heading angle. A convenient performance index is the sum of the characteristic velocities for deorbit, boost, and reorbit. Thus,

$$J = \Delta V_d + \Delta V_b + \Delta V_c \tag{14}$$

Where, ΔV_d, ΔV_b, and ΔV_c are the deorbit, boost, and reorbit characteristic velocities respectively, and are obtained from equations (2) and (11) as

$$\Delta V_d = \sqrt{\mu/R_d} - (R_a/R_d)V_e\cos(-\gamma_e) \tag{15}$$

$$\Delta V_c = \sqrt{\mu/R_c} - (R_a/R_c)(V_f+\Delta V_b)\cos\gamma_f \tag{16}$$

Alternatively, ΔV_d, ΔV_b and ΔV_c are also given by equations (3), (12), and (13) respectively. In the normalized form, the performance index becomes,

$$J = \Delta v = \Delta v_d + \Delta v_b + \Delta v_c \tag{17}$$

$$\Delta v_d = \sqrt{1/a_d} - (v_e/a_d)\cos(-\gamma_e) \tag{18}$$

$$\Delta v_c = \sqrt{1/a_c} - [(v_f+\Delta v_b)/a_c]\cos\gamma_f \tag{19}$$

where,

$$a_d = R_d/R_a; \quad a_c = R_c/R_a; \quad \Delta v_d = \Delta V_d/\sqrt{\mu/R_a}; \quad \Delta v_c = \Delta V_c/\sqrt{\mu/R_a}$$

Let us note that for a given circular orbit of radius R_c, the impulses ΔV_b and ΔV_c are completely determined by the velocity V_f and the flight path angle γ_f at the the atmospheric exit. The velocity V_e and the flight path angle γ_e at the entry point are dependent only on the magnitude of the deorbit impulse ΔV_d. For a specified atmospheric entry (i.e., for a given perigee altitude occurring within the atmosphere), we have a fixed value of ΔV_d and hence fixed values of entry velocity V_e, and entry flight path angle γ_e as seen from (1) and (2). Therefore, the optimal control problem for the minimum fuel consumption is confined only to the segment of the trajectory within the atmosphere. Hence, the performance index (14) is more appropriately written as

$$J = \Delta V_d + \Delta V_b(V_f, \gamma_f) + \Delta V_c(V_f, \gamma_f) \tag{20}$$

Ideally, as seen from equation (12), the minimum value of boost impulse ΔV_b is zero, when the exit velocity V_f is made equal to the perigee velocity of the exit-LEO elliptic orbit. Also, the minimum value of reorbit impulse ΔV_c is obtained when the vehicle exits with zero flight path inclination γ_f.

The first step in the optimization procedure using Pontryagin principle is to formulate the Hamiltonian as[2]

$$\mathcal{H} = \lambda_h bv\sin\gamma + \lambda_v\left\{- A_1 b(1+\eta^2)\delta v^2 - \frac{b^2\sin\gamma}{(b-1+h)^2}\right\}$$

$$+ \lambda_\gamma\left\{A_2 b\eta\delta v\cos\sigma + \frac{bv\cos\gamma}{(b-1+h)} - \frac{b^2\cos\gamma}{(b-1+h)^2 v}\right\}$$

$$+ \lambda_\phi\left\{\frac{bv\cos\gamma\sin\psi}{(b-1+h)}\right\}$$

$$+ \lambda_{\psi}\left\{\frac{A_2 b\delta\eta v\sin\sigma}{\cos\gamma} - \frac{bv\cos\gamma\cos\psi\tan\phi}{(b-1+h)}\right\} \tag{21}$$

where λ's are the costates corresponding to the states. The down range angle θ does not enter the right hand side of the equation (5) and hence need not be considered for the optimization process.

The optimal control equations for lift and bank angle are given by

$$\frac{\partial \mathcal{H}}{\partial \eta} = 0; \quad \frac{\partial \mathcal{H}}{\partial \sigma} = 0 \tag{22}$$

leading to

$$\eta = C_{LR}\omega/C_{DO}2v\lambda_v; \quad \tan\sigma = \lambda_{\psi}/\lambda_{\gamma}\cos\gamma \tag{23}$$

where

$$\omega = \sqrt{\lambda_{\gamma}^2 + \left(\lambda_{\psi}/\cos\gamma\right)^2} \tag{24}$$

The control C_L is bounded by the aerodynamic characteristics of the vehicle. Thus, for the constrained control,

$$|C_L| \leq C_{Lmax} \quad \text{or} \quad |\eta| \leq c_{max} \tag{25}$$

The costate (adjoint) equations are given by

$$\frac{d\lambda_h}{d\tau} = -\frac{\partial \mathcal{H}}{\partial h}; \qquad \frac{d\lambda_v}{d\tau} = -\frac{\partial \mathcal{H}}{\partial v}; \qquad \frac{d\lambda_{\gamma}}{d\tau} = -\frac{\partial \mathcal{H}}{\partial \gamma} \tag{26a}$$

$$\frac{d\lambda_{\phi}}{d\tau} = -\frac{d\mathcal{H}}{d\phi}; \qquad \frac{d\lambda_{\psi}}{d\tau} = -\frac{d\mathcal{H}}{d\psi} \tag{26b}$$

Boundary Conditions

The initial and final boundary conditions are given for the normalized altitude h as

$$h(\tau=0) = 1.0, \quad h(\tau=\tau_f) = 1.0 \tag{27a}$$

and for the normalized velocity v, and the flight path angle γ as

$$(2-v_e^2)a_d^2 - 2a_d + v_e^2\cos^2\gamma_e = 0 \tag{27b}$$

$$[2-(v_f+\Delta v_b)^2]a_c^2 - 2a_c + (v_f+\Delta v_b)^2\cos^2\gamma_f = 0 \tag{27c}$$

The equations (27b) and (27c) are obtained by eliminating ΔV_d from equations (1) and (2) and eliminating ΔV_c from equations (10) and (11) respectively. The remaining multiplier boundary conditions are obtained from the transversality conditions on the costates. Thus, the optimization procedure, requiring the solution of the state equations (8) and the costate equations (26) along with the boundary conditions given by equation (27) leads to a nonlinear TPBVP, which can only be solved by numerical methods.

Multiple Shooting Method

The multiple shooting method is a powerful method for solving nonlinear TPBVP.[8-10] In solving any boundary value problem with the given initial and final conditions, we assume additional initial data and integrate forward so that the solution satisfies the given final condition as well. This is also called a simple shooting method. However, the convergence of the solution is highly sensitive to the assumed initial data. The error due to inaccurate initial data can be made arbitrarily small by performing the integration over sufficiently smaller subdivided panels within the given interval and thereby

leading to the multiple shooting method. Thus, the multiple shooting method is a simultaneous application of the simple shooting method at several points within the interval of integration. Here, the trajectory may be restarted at intermediate points using new guesses. Jacobian matrices are formed for each segment. The resulting iteration scheme, based on reducing all discontinuities at internal grid points to zero, leads to a system of linear algebraic equations. The corresponding OPTSOL code, developed by Deutsche Forschungs-und Versuchsanstalt fur Luft-und Raumfahrt (DFVLR) at Oberpfaffenhofen, West Germany, was used for solving the present problem.

IV. NUMERICAL DATA AND RESULTS

A typical AOTV configuration[12] with L/D of about 1.5 is shown in Fig. 4. The liquid oxygen is stored in two separate tanks to provide a tapered nose, and inflated chins are used to continue this tapering along the body. A large deployable flap is provided to trim the vehicle at low angles of attack for maximum L/D performance. A representative set of numerical values used for a complete mission from GEO to SSO at an altitude of 556 km is given below.[3,6]

$C_{DO} = 0.1$; $K = 1.11$; $m/S = 300\ kg/m^2$

$\rho_s = 1.225\ kg/m^3$; $\mu = 3.96772 \times 10^{14}\ m^3/sec^2$

$\beta = 1/6900\ m^{-1}$; $R_E = 6356.766\ km$

$H_a = 120\ km$; $R_d = 42240.766\ km$; $R_c = 6912.766\ km$

Using the above mentioned data, the optimal solution has the following entry and exit status.

Entry status: $H_e = 120\ km$; $V_e = 10305.58\ m/sec$

$\gamma_e = -6.0$ degrees; $\phi_e = 0$; $\psi_e = 0$

Exit status: H_f = 120 km; V_f = 7462.35 m/sec

γ_f = 0.1595 deg; ϕ_f = 11.95 deg

ψ_f = 24.1 deg; total flight time = 520 sec

Characteristic velocities:

Deorbit characteristic velocity, ΔV_d = 1493.32 m/sec

Boost characteristic velocity, ΔV_b = 490.77 m/sec

Reorbit characteristic velocity, ΔV_c = 124.61 m/sec

Total characteristic velocity ΔV = 2108.7 m/sec

The complete mission in terms of the velocity profile is shown in Fig. 5. Initially, the vehicle is in a circular orbit at GEO moving at a speed V_d = 3064.82 m/sec. A deorbit impulse ΔV_d = 1493.32 m/sec is executed to fly the vehicle along the GEO-entry elliptic orbit. The elliptic velocity at the deorbit point D is $\bar{V}_d = V_d - \Delta V_d$ = 1571.5 m/sec. At the atmospheric interface E of altitude H_a = 120 km, the vehicle attains an orbital velocity V_e = 10305.58 m/sec. During the atmospheric maneuver, the velocity of the vehicle is depleted and the exit velocity is V_f = 7462.35 m/sec. In order to attain the desired SSO altitude H_c = 556 km, a boost impulse ΔV_b = 490.77 m/sec is required at the exit F from the atmosphere. Then the elliptic velocity at the exit is $\bar{V}_f = V_f + \Delta V_b$ = 7953.12 m/sec. The vehicle travels then along the exit-SSO elliptic path and has a velocity $\bar{V}_c$ = 7451.47 m/sec at the reorbit point C. In order to insert the vehicle into a circular orbit at this altitude H_c = 556 km, a reorbit impulse ΔV_c = 124.61 m/sec is imparted. The vehicle is now in a circular orbit at SSO moving with a speed of $V_c = \bar{V}_c + \Delta V_c$ = 7576.08 m/sec.

Fig. 6(a) shows the time history of altitude. The spacecraft enters and exits the atmosphere at the altitude of 120 km. The minimum altitude reached is 44.72 km. Fig. 6(b) shows a velocity reduction of 2843.23 m/sec. The profile of flight path angle with time is shown in Fig. 6(c). The spacecraft enters the atmosphere with an inclination of -6.00 degrees and exits with 0.1595 degrees. The time history of cross range ϕ is shown in Fig. 6(d) which has a value of 11.95 degrees at the end of the atmospheric maneuver. Fig. 6(e) shows the variation of heading angle ψ, which shows that the atmospheric maneuver provides an orbital inclination of 24.1 degrees.

The control history is shown in Fig. 7(a). The vehicle enters the atmosphere with maximum lift capability and decreases slowly during the remaining flight. Fig. 7(b) shows the variation of bank angle during the atmospheric flight. Initially the vehicle enters the atmosphere with a bank angle of 144.5 degrees to pull the vehicle into the atmosphere but slowly drops to about 75 degrees and maintain at a value of 96 degrees for most of the remainder of the flight. The lift-to-drag ratio is shown in Fig. 7(c). Fig. 8(a) shows the peak heating rate of 402.64 W/sq. cm. As shown in Fig. 8(b), the peak dynamic pressure is 80.73 KN/sq. m.

Fig. 9 shows the successive approximations of the altitude H, during the course of 0, 15, and 30 iterations in using the multiple shooting method. For the sake of clarity only 4 out of 20 intervals are shown. The initial guessed value for the altitude is 120 km at every interval. It can be seen how the initially large jumps at the subdivision points are "flattened out" with the increase of iterations.

V. CONCLUDING REMARKS

In this paper, we have addressed the problem of minimization of fuel consumption during the atmospheric portion of an aeroassisted, orbital transfer with plane change. The complete mission has required three characteristic velocities, a deorbit impulse at HEO, a boost impulse at the atmospheric exit, and a reorbit impulse at LEO. A performance index has been formulated as the sum of these three impulses. Application of optimal control principles has led to a nonlinear, two-point, boundary value problem which was solved by using a multiple shooting algorithm. The strategy for the atmospheric portion of the minimum-fuel transfer is to start initially with the maximum positive lift in order to recover from the downward plunge, and then to fly with a gradually decreasing lift such that the vehicle skips out of the atmosphere with a flight path angle near zero degrees.

Acknowledgements

This research work was supported by the grant NAG1-736 from Spacecraft Control Branch, NASA Langley Research Center, Hampton.

VI. REFERENCES

1. Walberg, G. D., "A Survey of Aeroassisted Orbital Transfer," J. Spacecraft, 22, pp. 3-18, Jan.-Feb. 1985.

2. Vinh, N.-X., Optimal Trajectories in Atmospheric Flight, Elsevier Scientific Publishing Co., Amsterdam, 1981.

3. Dickmann, E. D., "The Effect of Finite Thrust and Heating Constraints on the Synergetic Plane Change Maneuver for Space-Shuttle Orbiter-Class

Vehicle," NASA TN D-7211, Oct. 1973.

4. Hull, D. G., Glitner, J. M., Speyer, J. L., and Maper, J., "Minimum Energy Loss Guidance for Aeroassisted Orbital Plane Change," J. Guidance, Control, and Dynamics, 8, pp. 487-493, July-Aug. 1985.

5. Vinh, N. X., and Hanson, J. M., "Optimal Aeroassisted Return from High Earth Orbit with Plane Change," Acta Astronautica, 12, pp. 11-25, Jan. 1985.

6. Miele, A., Baspur, V. K., and Lee, W. Y., "Optimal Trajectories for Aeroassisted Noncoplanar Orbital Transfer," Acta Astronautica, 15, pp. 399-412, June-July 1987.

7. Mishne, D., and Speyer, J. L., "Optimal Control of Aeroassisted Plane Change Maneuver using Feedback Expansions," Proc. AIAA Flight Mechanics Conf., Williamsburg, Aug. 1986.

8. H. B. Keller, Numerical Methods for Two-Point Boundary-Value Problems, Blaisdell Publ. Co., Waltham, 1968.

9. Stoer, J., and Bulirsch, R., Introduction to Numerical Analysis,, Springer-Verlag, New York, 1980.

10. Pesch, H. J., "Numerical Computation of Neighboring Optimum Feedback Control Schemes in Real-Time," Appl. Math. Optim., 5, pp. 231-252, 1979.

11. Marec, J. P., Optimal Space Trajectories, Elsevier Scientific Publishing Company, Amsterdam, 1979.

12. Talay, T. D., White, N. H., and Naftel, J. C., "Impact of Atmospheric Uncertainties and Viscous Interaction Effects on the Performance of Aeroassisted Orbital Transfer Vehicles," AIAA 22nd Aerospace Science Meeting, Reno, NV, Jan. 9-12, 1984.

****

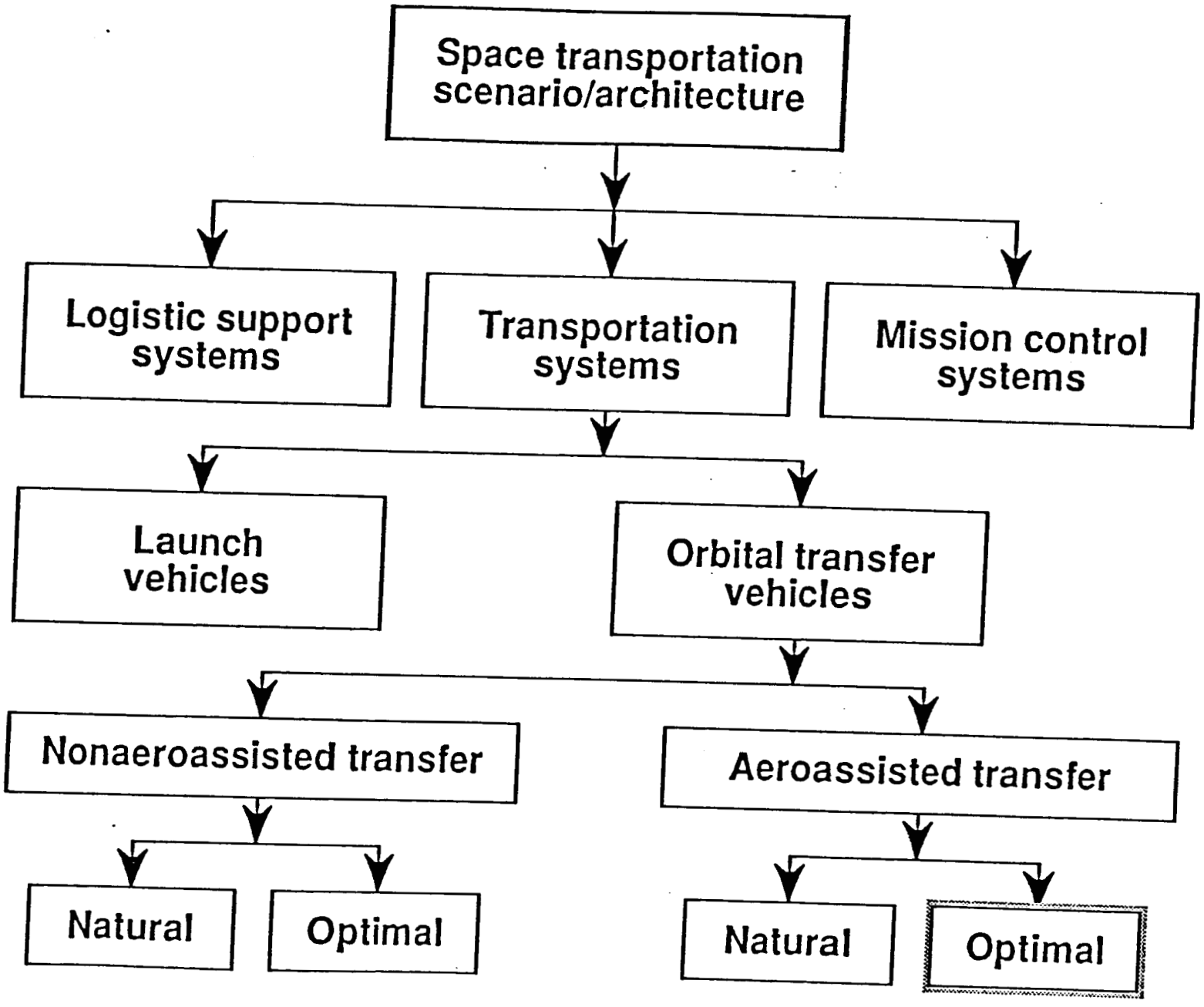

Fig. 1 Space transportation architecture

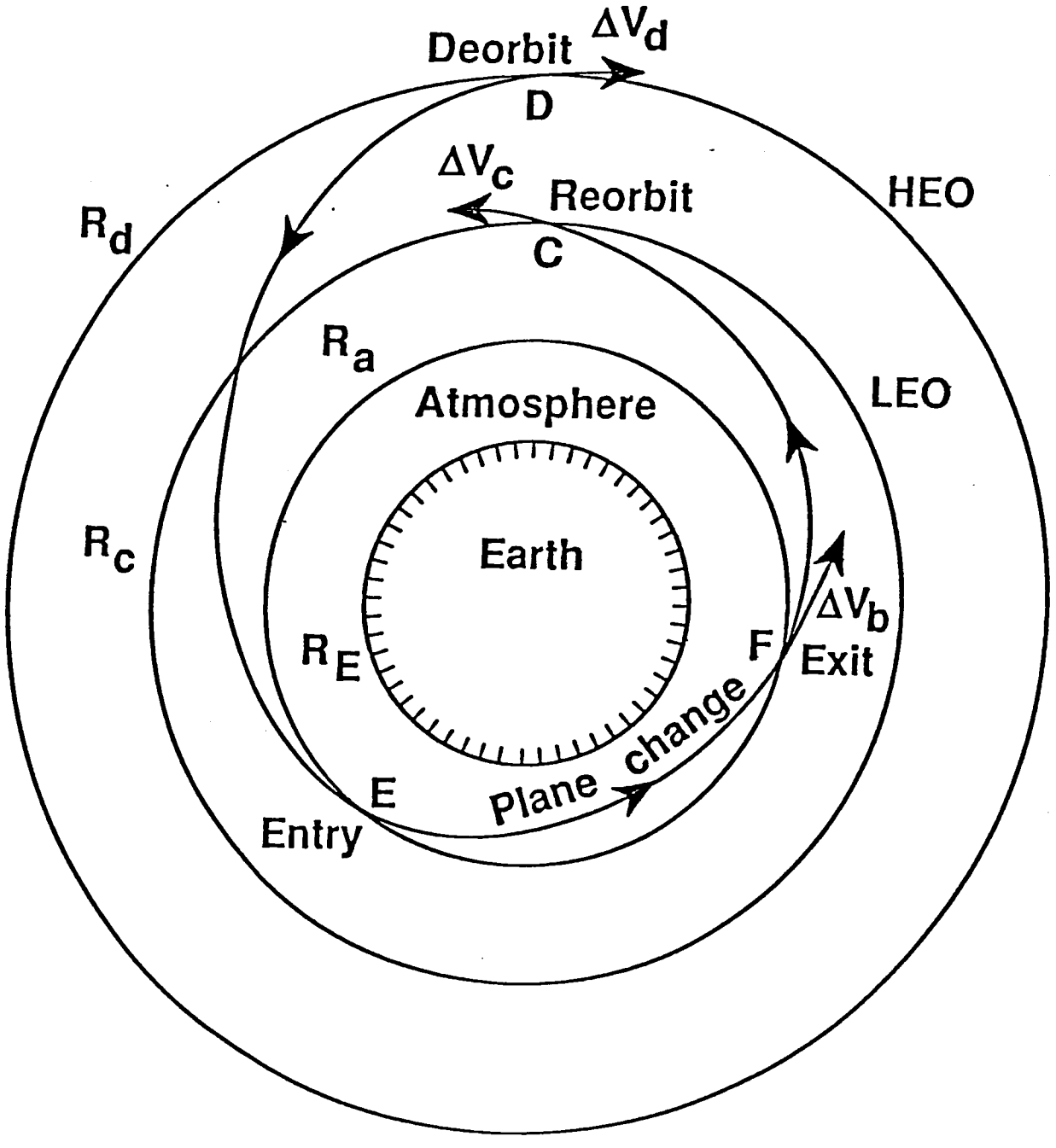

Fig. 2 Aeroassisted orbital plane change

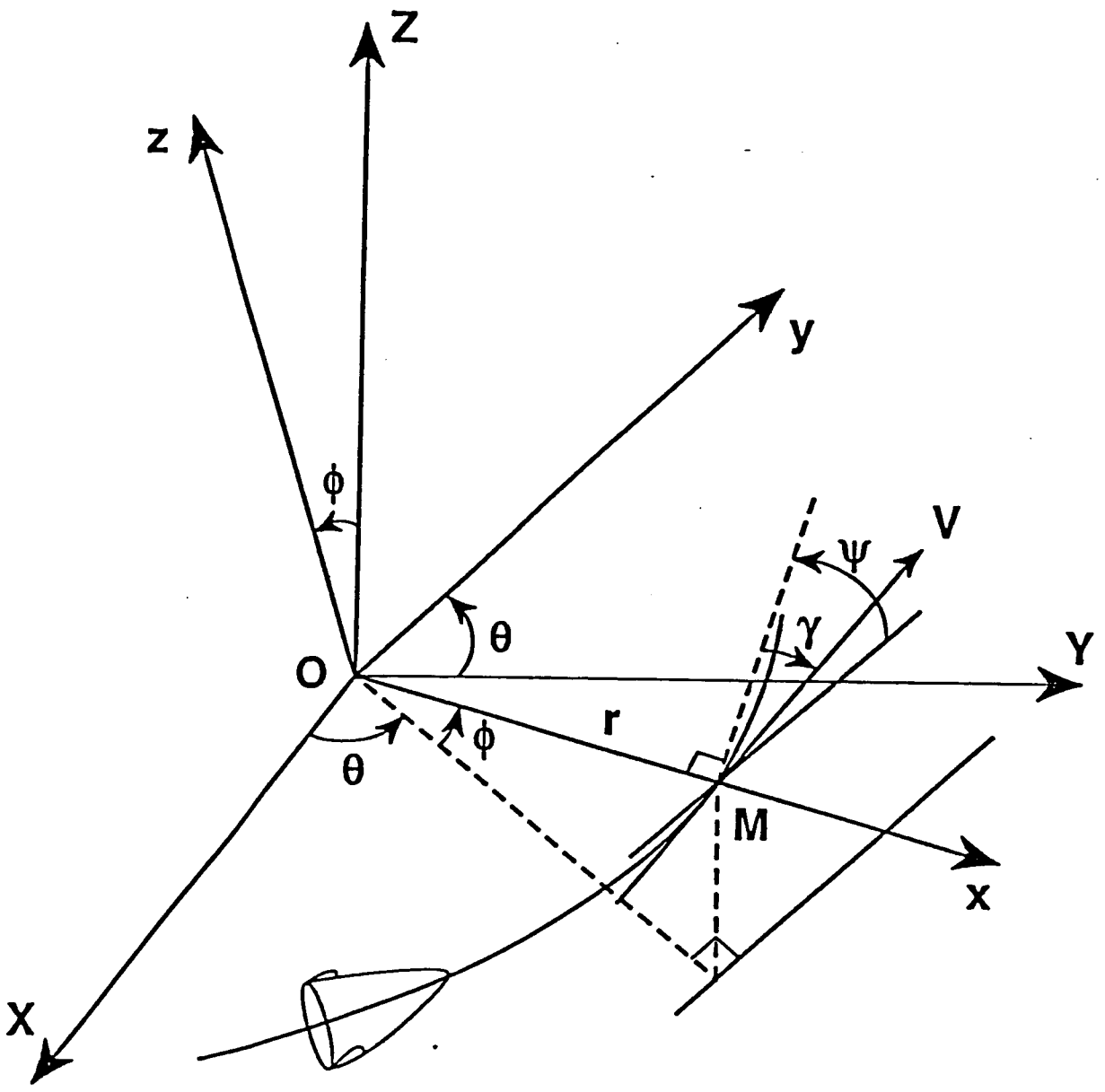

Fig. 3 Coordinate system

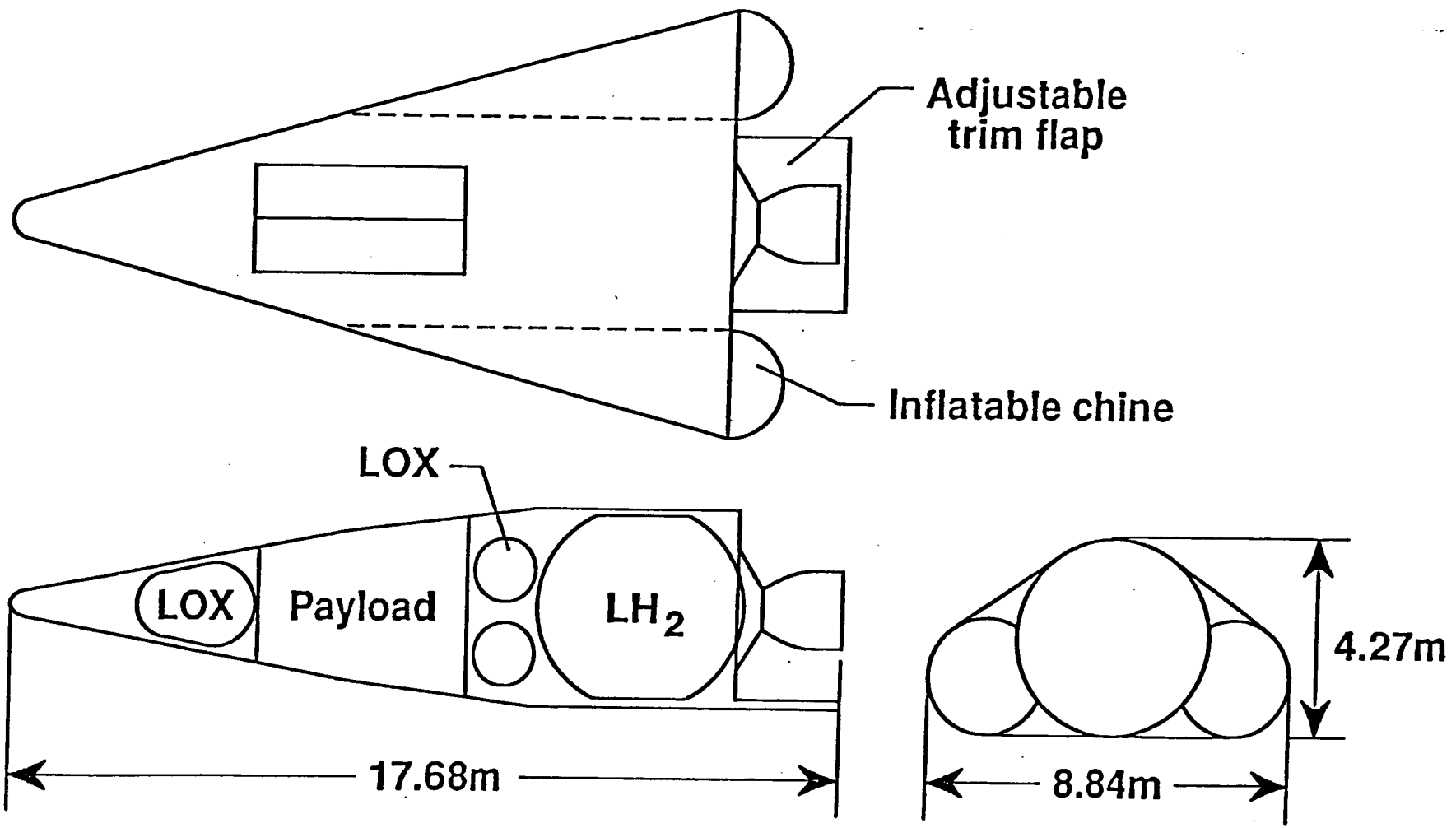

Fig. 4 Vehicle configuration

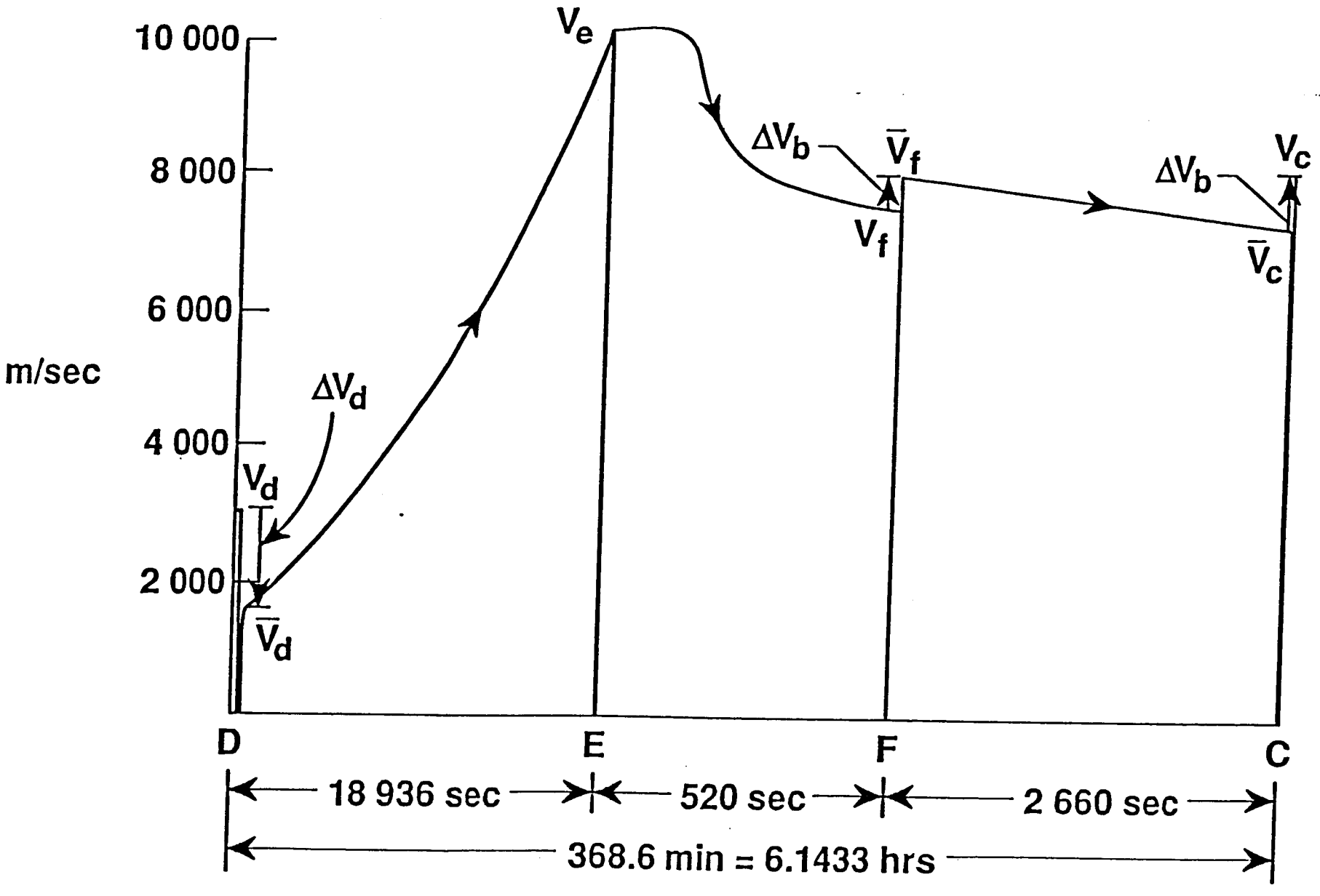

Fig. 5 Velocity profile for complete mission.

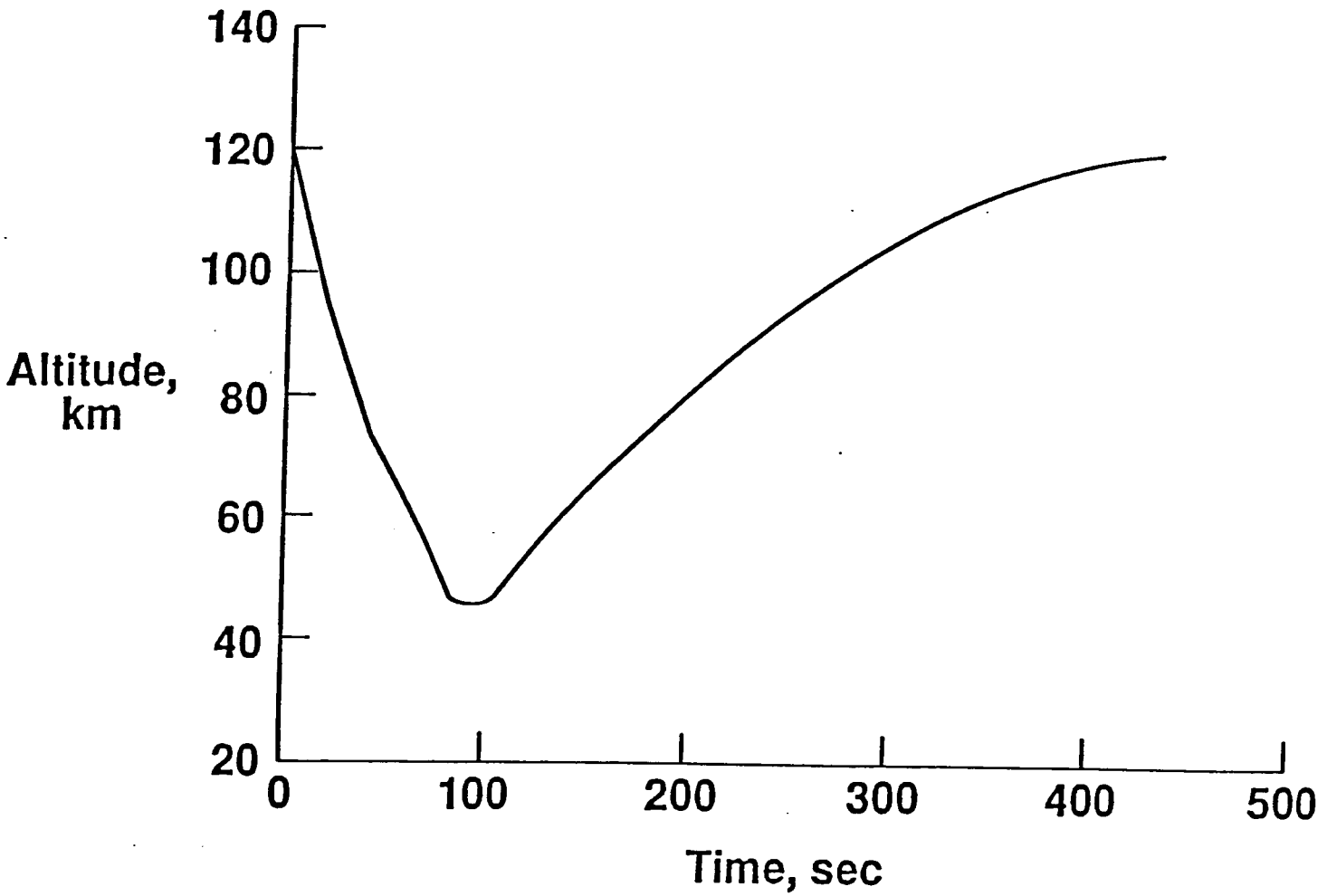

Fig. 6(a) Time history of altitude

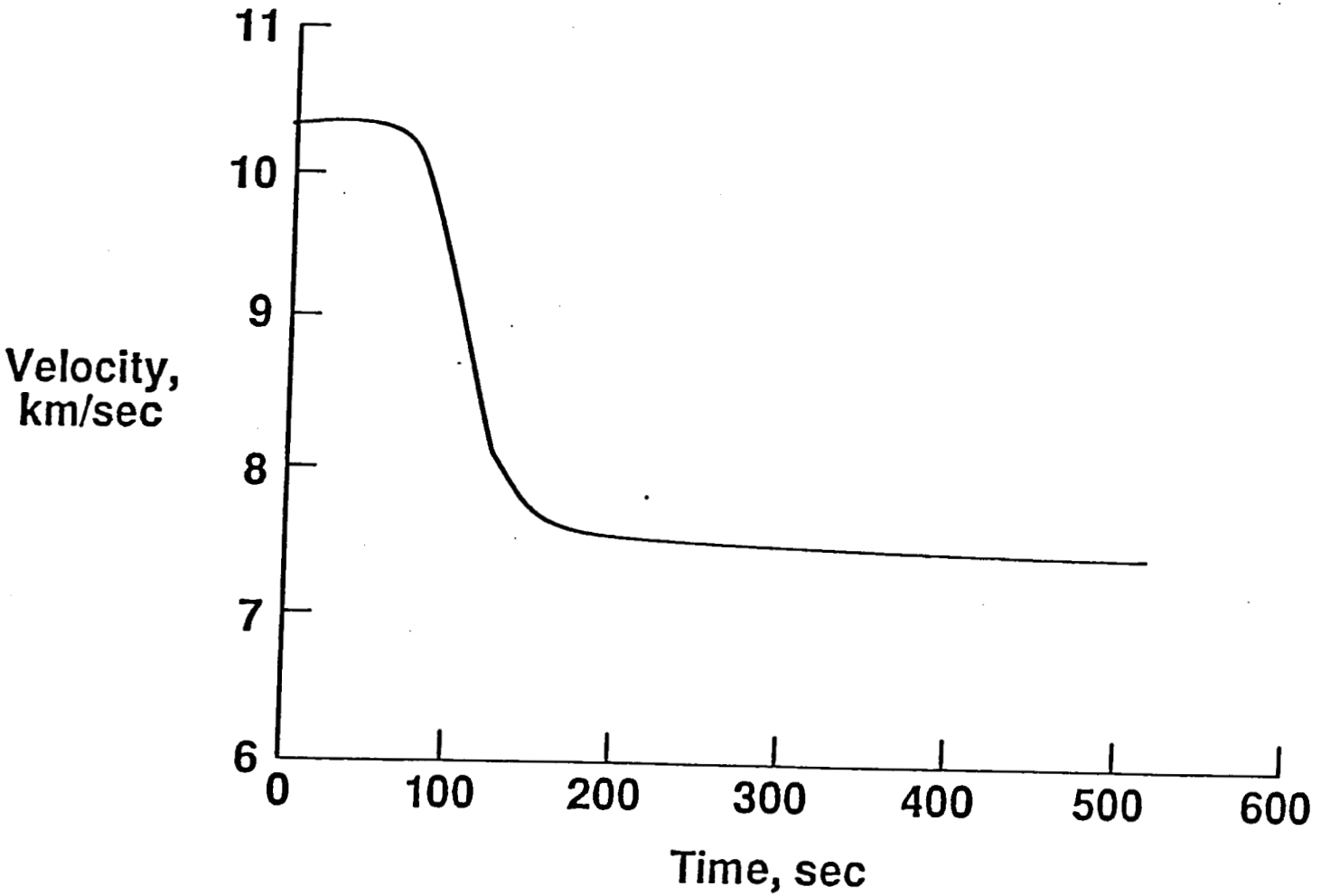

Fig. 6(b) Time history of velocity

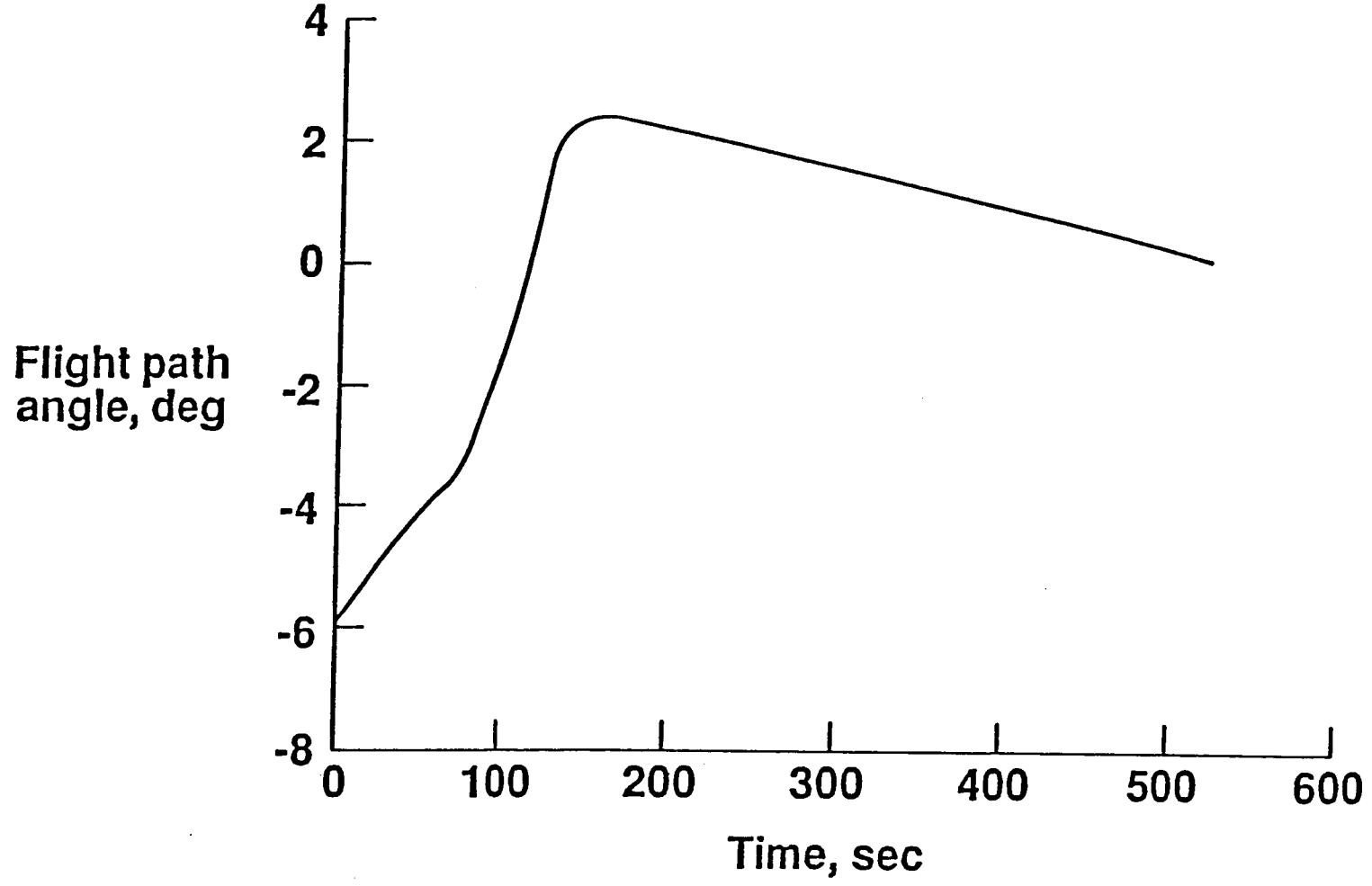

Fig. 6(c) Time history of flight path angle

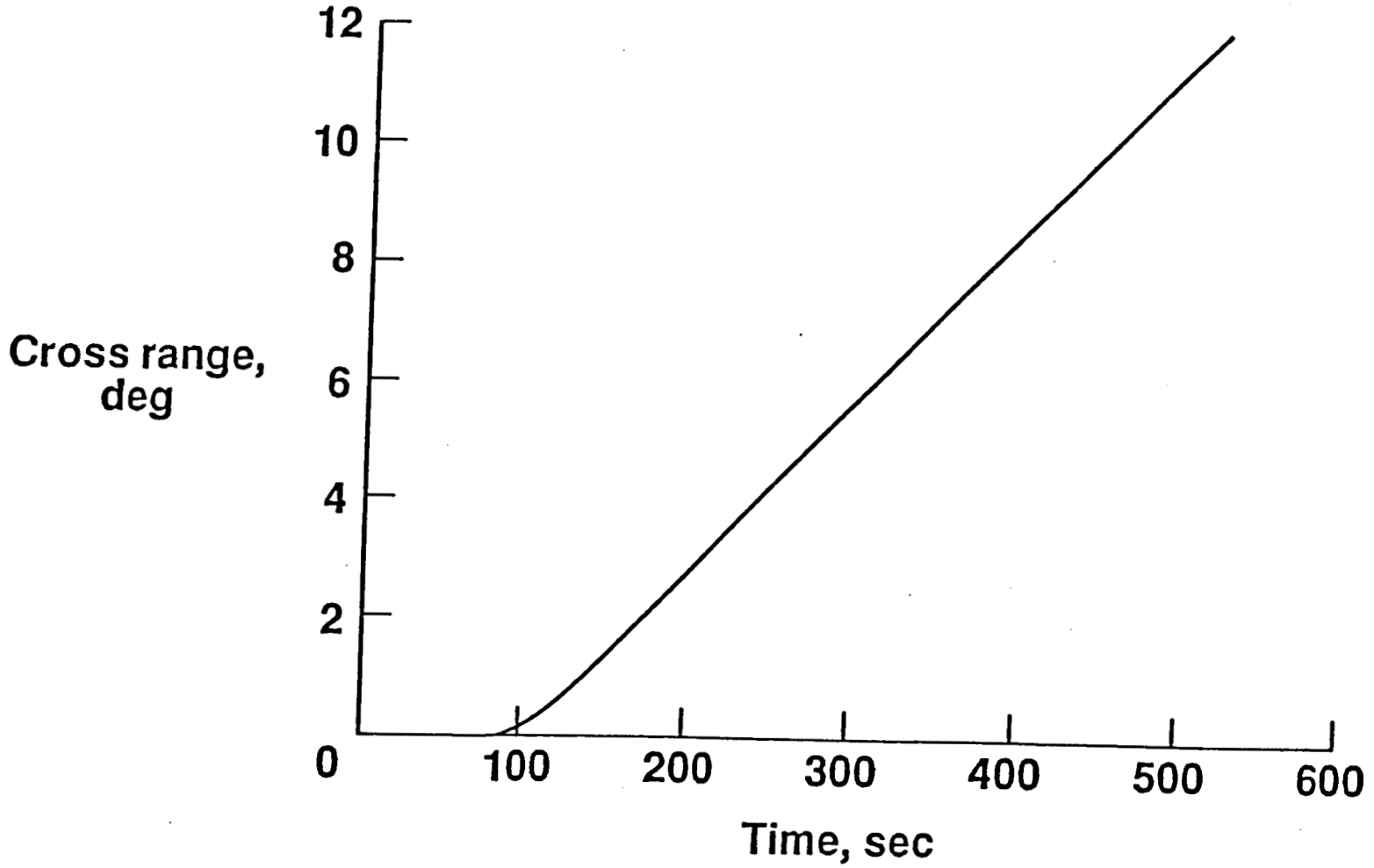

Fig. 6(d) Time history of cross range

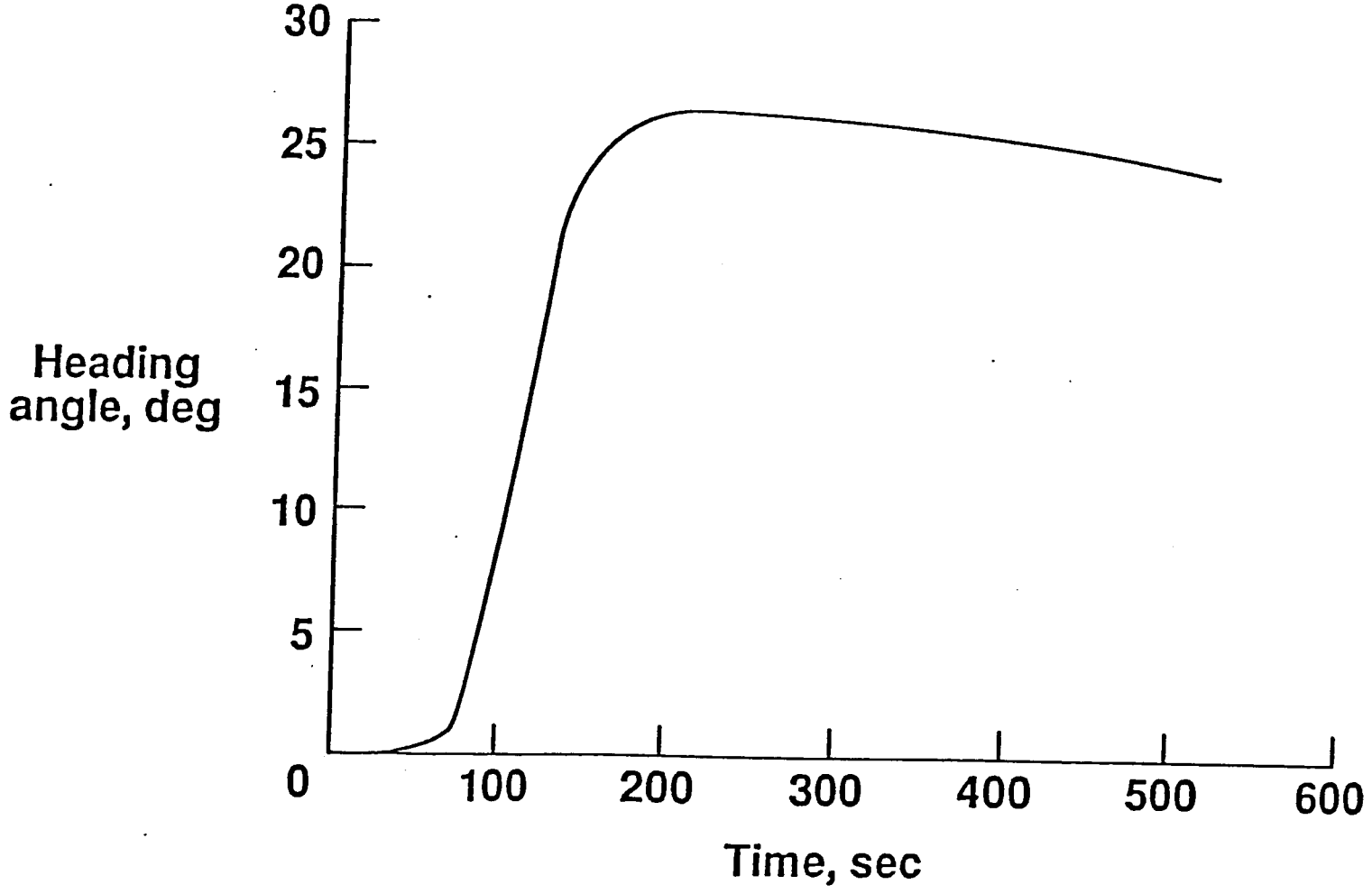

Fig. 6(e) Time history of heading angle

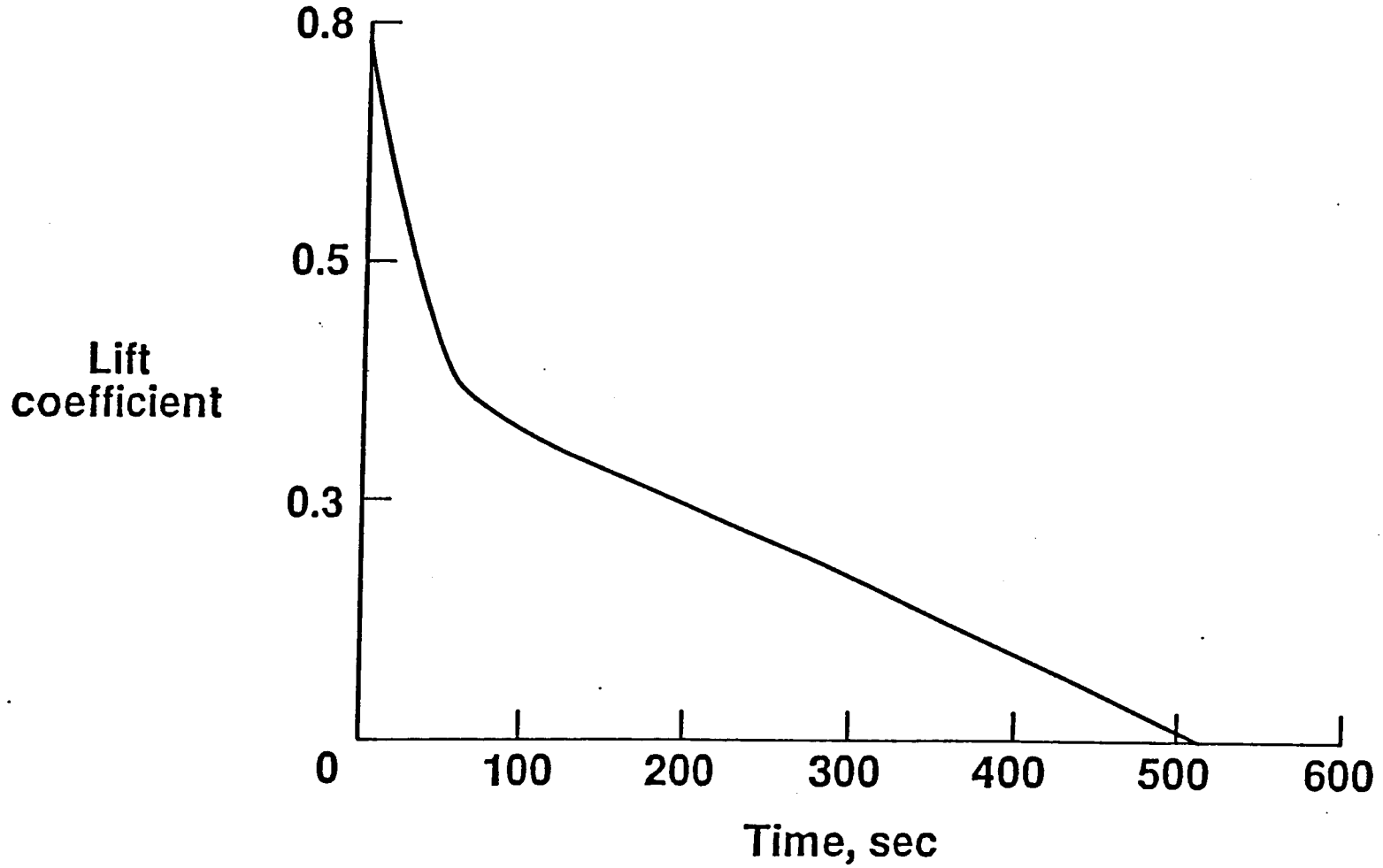

Fig. 7(a) Time history of lift coefficient

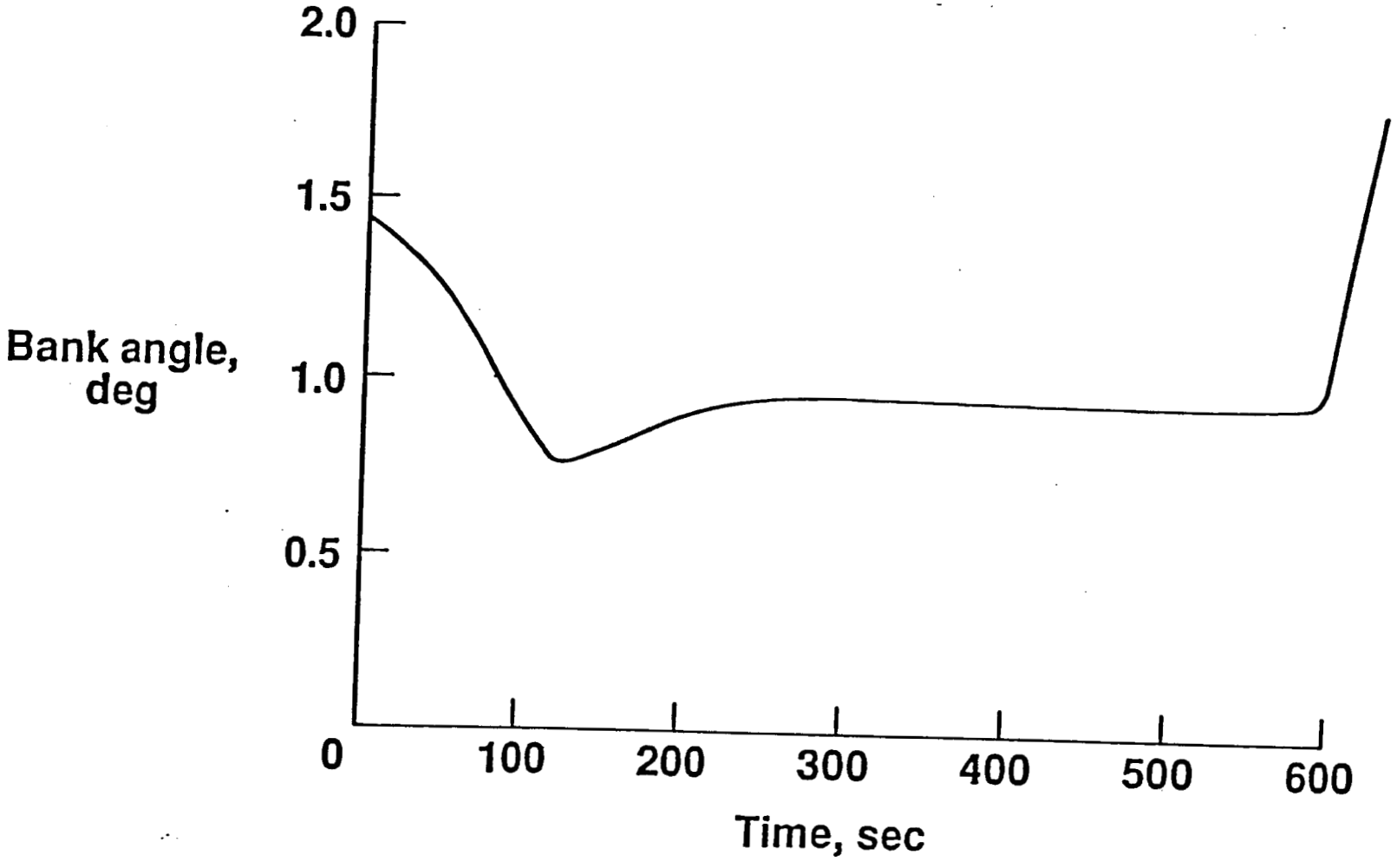

Fig. 7(b) Time history of bank angle

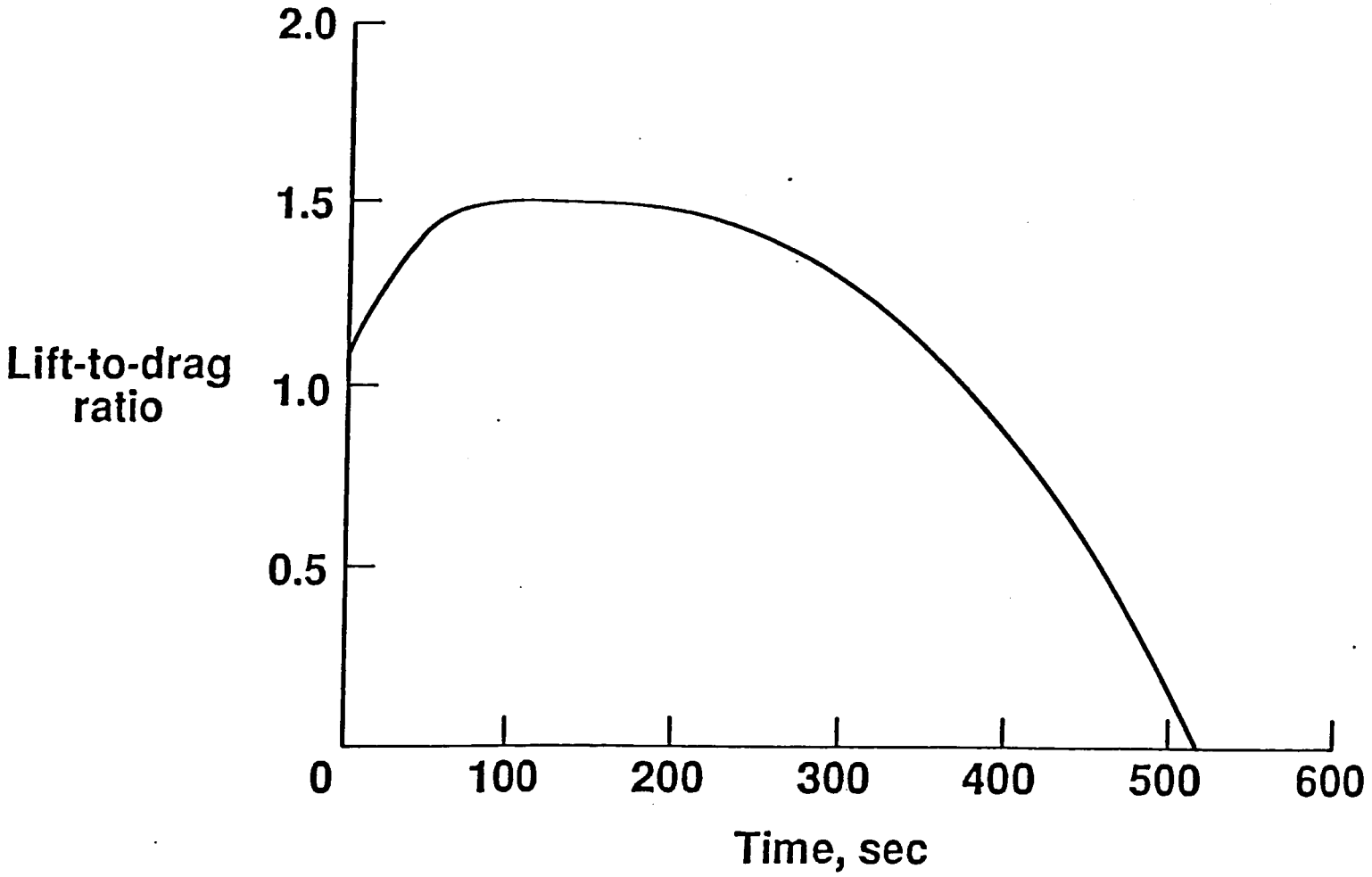

Fig. 7(c) Time history of lift-to-drag ratio

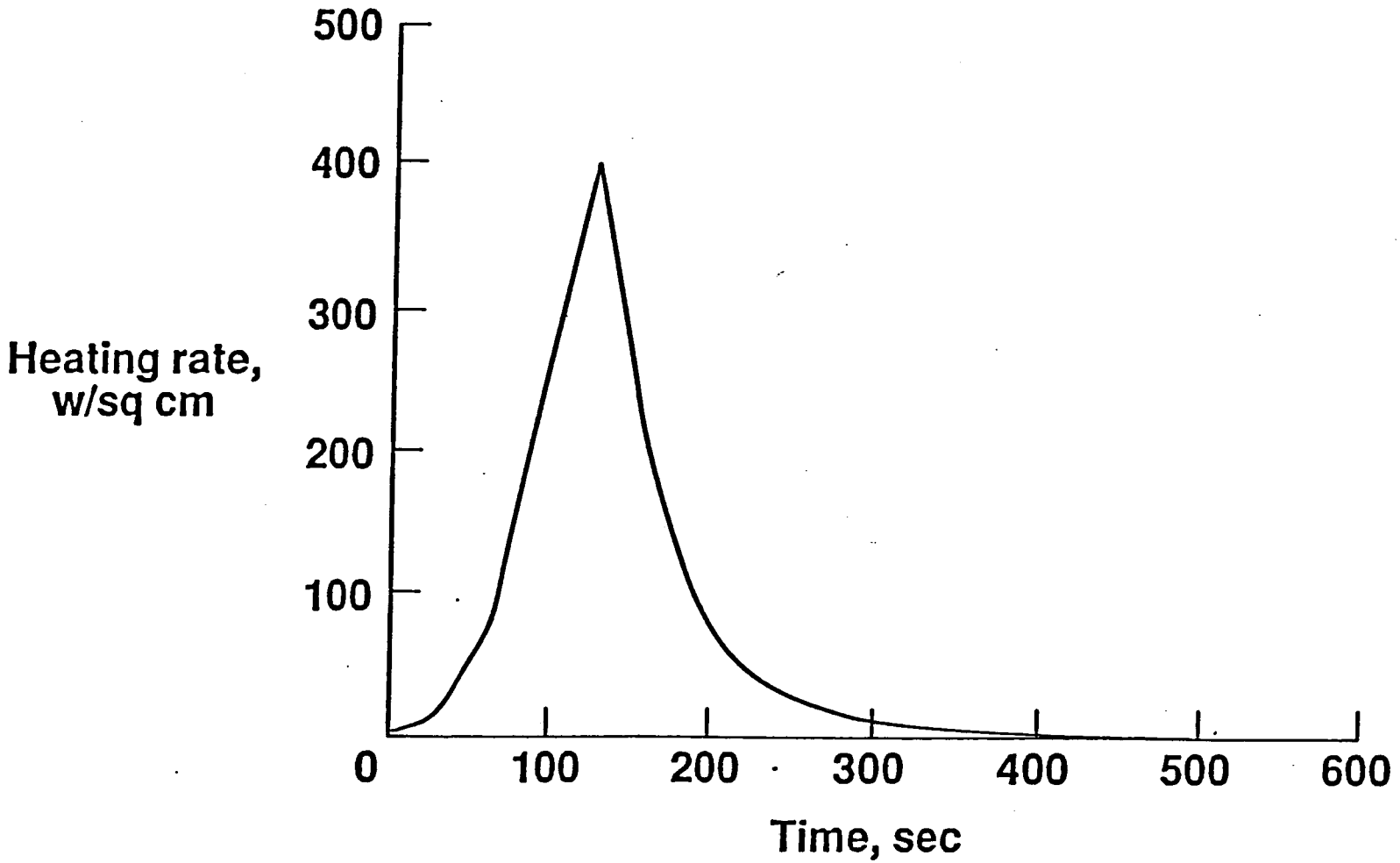

Fig. 8(a) Time history of heating rate

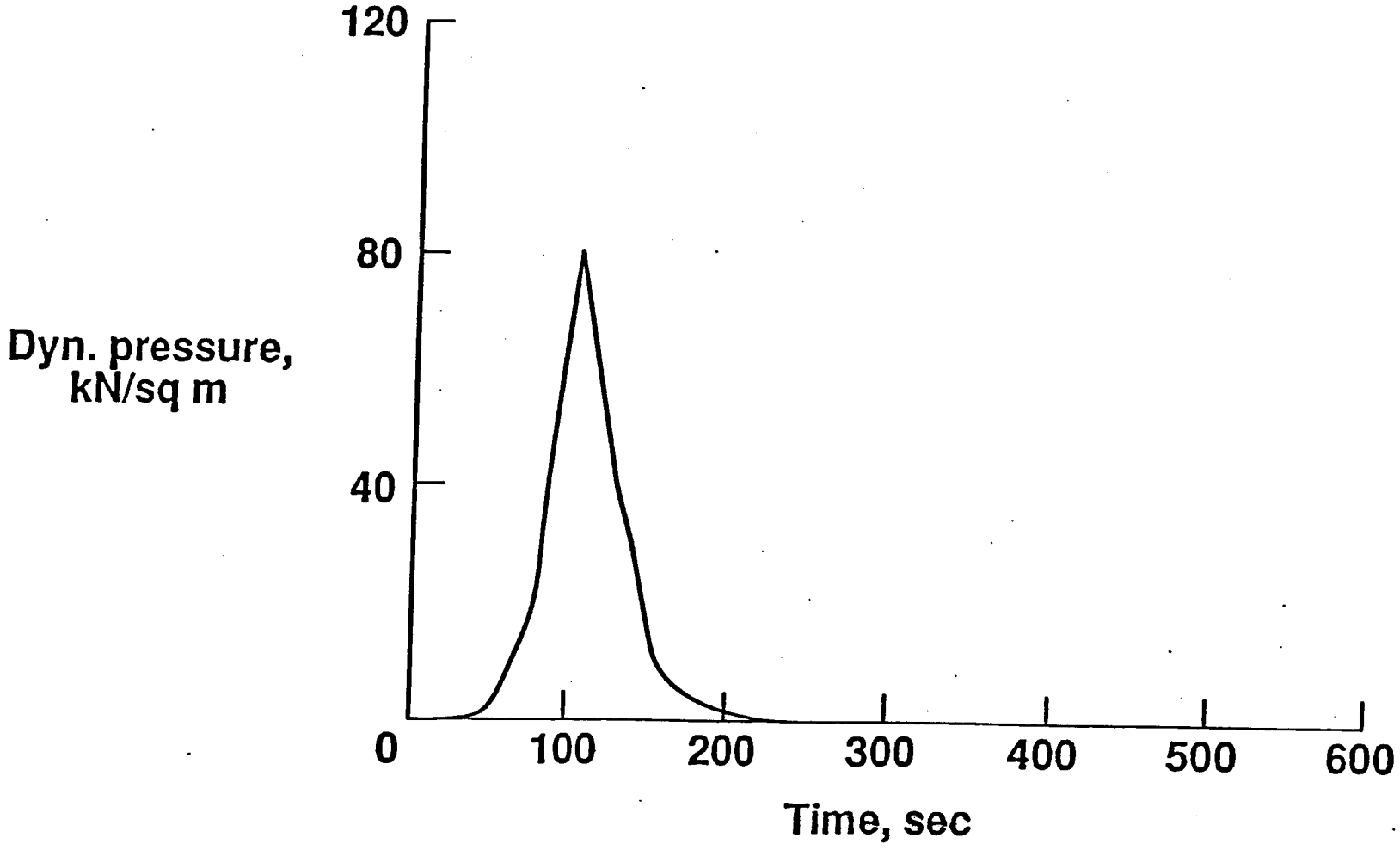

Fig. 8(b) Time history of dynamic pressure

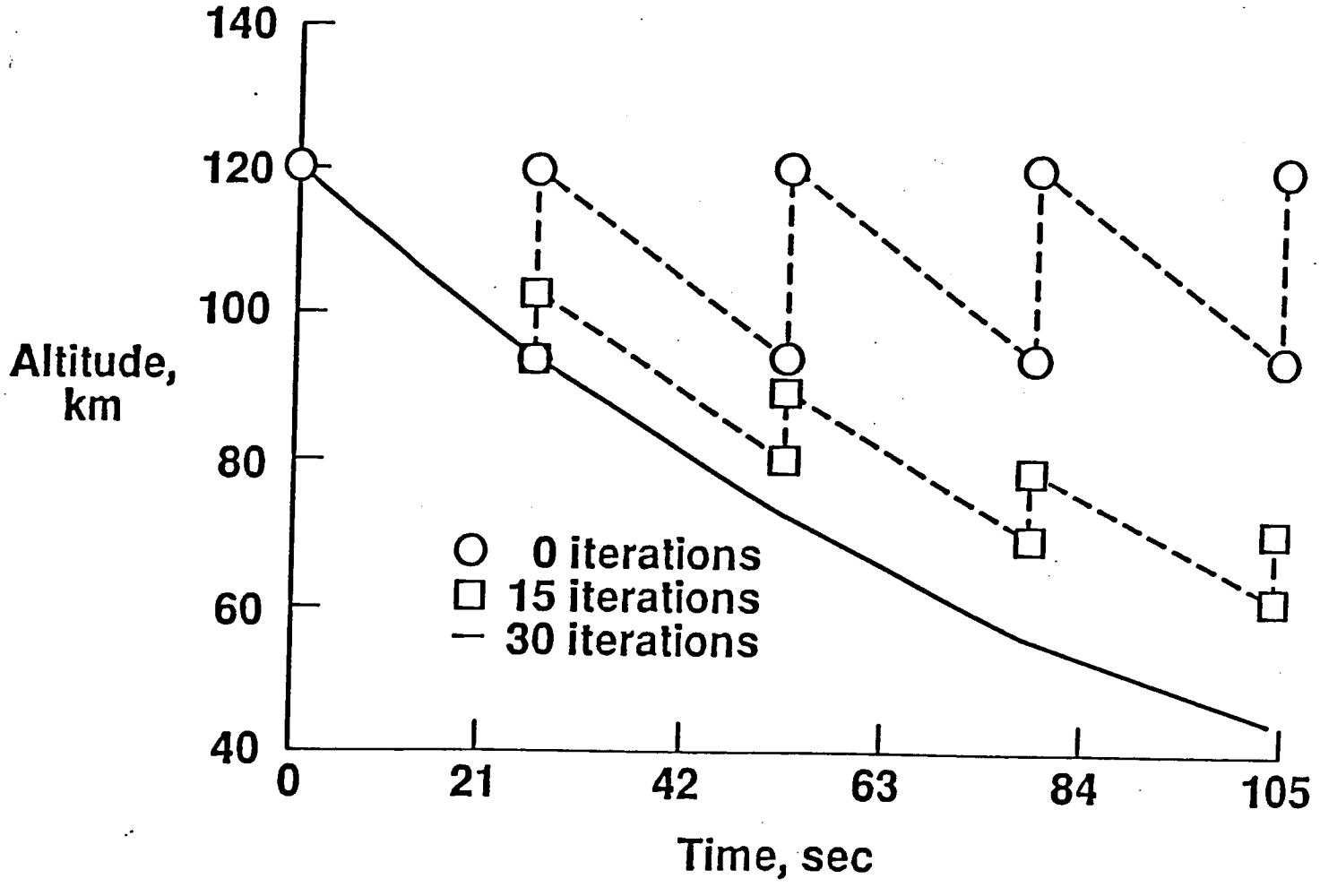

Fig. 9 Successive approximations for altitude

FUEL-OPTIMAL TRAJECTORIES FOR AN AEROASSISTED ORBITAL TRANSFER VEHICLE

Dr. D. S. Naidu
ODU Research Foundation
Spacecraft Control Branch, MS 161
NASA Langley Research Center
Hampton, VA, 23665-5225

TABLE OF CONTENTS

ABSTRACT: The fuel-optimal problem in noncoplanar orbital transfer employing aeroassist technology is addressed. The mission involves the transfer from high Earth orbit to low Earth orbit with plane change. The complete maneuver consists of a deorbit impulse to inject a vehicle from a circular orbit to elliptic orbit to enter the atmosphere, a boost impulse at the exit from the atmosphere for the vehicle to attain a desired orbital altitude and finally a reorbit impulse to circularize the path of the vehicle. In order to minimize the total fuel consumption, a performance index is chosen as the sum of the deorbit, boost, and reorbit impulses. For a typical aeroassisted orbital transfer vehicle with high lift-to-drag ratio, the simulations are carried out using the industry standard POST program.

NOMENCLATURE

AOTV: aeroassisted orbital transfer vehicle

GEO: geosynchronous Earth orbit

H : altitude

HEO: high Earth orbit

J : performance index

LEO: low Earth orbit

OTV: orbital transfer vehicle

R : distance from Earth center to vehicle center of gravity

R_E : radius of Earth

SSO: space station orbit

V : velocity

γ : flight path angle

ΔV : characteristic velocity

Subscripts

a : atmospheric boundary

c : circularization or reorbit at LEO

d : deorbit at HEO

e : entry to atmosphere

f : exit from atmosphere

1. INTRODUCTION

The main function of the space transportation system is to deliver payloads from Earth to various locations in space. Until now, this function has been performed by various rockets, the space shuttle, and expendable upper stages using solid or liquid propellants. In particular, considering the economic benefits and reusability, an orbital transfer vehicle (OTV) is proposed for transporting payloads between low Earth orbit (LEO) and high Earth orbit (HEO). The two basic operating modes contemplated for OTV are a ground-based OTV which returns to Earth after each mission and a space-based OTV which operates out of an orbiting hanger located at the proposed Space Station.

In a typical mission, a space-based OTV, which is initially at the space station orbit (SSO), is required to transfer a payload to geosynchronous Earth orbit (GEO), pick up another payload, say a faulty satellite, and return to rendezvous with the orbiting hanger at SSO for refurbishment and redeployment of the payload. The OTV on its return journey from GEO to SSO needs to dissipate some of its orbital energy. This can be accomplished by using an entirely propulsive (Hohmann) transfer in space only or a combination of propulsive transfer in space and aeroassisted maneuver in the atmosphere. It

has been established that a significant fuel savings and hence increased payload capabilities can be achieved with propulsive and aeroassisted maneuvers instead of all-propulsive maneuvers[1]. This leads to an aeroassisted orbital transfer vehicle (AOTV), which on its return leg of the mission, dips into the Earth's atmosphere, utilizes atmospheric drag to reduce the orbital velocity and employs lift and bank angle modulations to achieve a desired orbital inclination. Basically, the AOTV performs a synergetic maneuver, employing a hybrid combination of propulsive maneuver in space and aerodynamic maneuver in the atmosphere.

It is believed that the concept of aeroassisted orbital transfer opens new mission opportunities for the space transportation system, especially with regard to the establishment of the permanent space station. Fig. 1 shows the space transportation architecture relevant to aeroassist technology. The optimization of fuel is an important aspect of orbital transfer missions[2-7].

In this paper, we address the fuel-optimal problem arising in noncoplanar orbital transfer employing aeroassist technology. The maneuver involves the transfer from HEO to LEO with a plane change and at the same time minimization of the fuel consumption. It is known that the change in velocity, also called the characteristic velocity, is a convenient measure of the fuel consumption. For minimum-fuel maneuver, the objective is then to minimize the total characteristic velocity for deorbit, boost, and reorbit (or circularization). For a typical AOTV with high L/D capability, the simulations are carried out using the industry standard Program to Optimize Simulated Trajectories (POST)[8]. Fuel-optimal trajectories are obtained for the given atmospheric entry, orbital inclination, and LEO altitude.

2. MISSION DESCRIPTION

The complete mission from HEO to LEO with atmospheric pass is depicted in Fig. 2. It is composed of three impulses: first, a deorbit impulse ΔV_d at HEO to inject the vehicle into a HEO-entry elliptic orbit, second, a boost impulse ΔV_b at the exit from the atmosphere for the vehicle to attain sufficient velocity to travel along an exit-LEO elliptic orbit, and finally, a circularizing impulse ΔV_c to circularize the path of the vehicle.

Consider the different phases of deorbit, aeroassist (or atmospheric flight), boost and reorbit (or circularization).

Deorbit

Initially, we assume that the spacecraft is in a circular orbit of radius R_d, well outside the Earth's atmosphere, moving with a circular velocity $V_d = \sqrt{\mu/R_d}$. Deorbit is performed by means of an impulse ΔV_d, to transfer the vehicle from the circular orbit to elliptic orbit with perigee low enough to intersect the dense part of the atmosphere [Fig. 2]. Since the elliptic velocity at D is less than the circular velocity at D, the impulse ΔV_d is executed so as to oppose the circular velocity V_d. In other words, at point D, the velocity required to put the vehicle into elliptic orbit is less than the velocity required to maintain it in circular orbit. The deorbit impulse ΔV_d causes the vehicle to enter the atmosphere of radius R_a with a velocity V_e and flight path angle γ_e. It is known that the optimal-energy loss maneuver from the circular orbit is simply the Hohmann transfer and the impulse is parallel and opposite to the instantaneous velocity vector.

Using the principle of conservation of energy and angular momentum at the deorbit point D, and the atmospheric entry point E, we get[9],

$$V_e^2/2 - \mu/R_a = (V_d-\Delta V_d)^2/2 - \mu/R_d \quad (1)$$

$$R_a V_e \cos(-\gamma_e) = R_d(V_d-\Delta V_d) \quad (2)$$

from which solving for ΔV_d, we get

$$\Delta V_d = \sqrt{\mu/R_d} - \sqrt{2\mu(1/R_a-1/R_d)/[(R_d/R_a)^2/\cos^2\gamma_e-1]} \quad (3)$$

It is easily seen that the minimum value of the deorbit impulse ΔV_{dm} obtained at $\gamma_e = 0$, corresponds to an ideal transfer with the space vehicle grazing the atmospheric boundary. To ensure proper atmospheric entry, deorbit impulse ΔV_d must be higher than the minimum deorbit impulse ΔV_{dm} which is given by

$$\Delta V_{dm} = \sqrt{\mu/R_d} - \sqrt{2\mu(1/R_a-1/R_d)/[(R_d/R_a)^2-1]} \quad (4)$$

Aeroassist, Boost, and Reorbit

During the aeroassist (or atmospheric) flight, the vehicle is controlled by bank angle with a constant angle of attack to achieve the necessary velocity reduction (due to atmospheric drag) and the plane change. Due to the loss of energy during the atmospheric flight, a second impulse is required to boost the vehicle back to orbital altitude.

The vehicle exits the atmosphere at point F, with a velocity V_f and flight path angle γ_f. The additional impulse ΔV_b, required at the exit point F for boosting into an elliptic orbit with apogee radius R_c and the reorbit

impulse ΔV_c required to insert the vehicle into a circular orbit at point C, are obtained by using the principle of conservation of energy and angular momentum at the exit point F, and the circularization point C. Thus, we have,

$$(V_f+\Delta V_b)^2/2 - \mu/R_a = (V_c-\Delta V_c)^2/2 - \mu/R_c \tag{5}$$

$$(V_f+\Delta V_b)R_a\cos\gamma_f = R_c(V_c-\Delta V_c) \tag{6}$$

Solving for ΔV_b and ΔV_c from the above equations (5) and (6),

$$\Delta V_b = \sqrt{2\mu(1/R_a-1/R_c)/\left[1-(R_a/R_c)^2\cos^2\gamma_f\right]} - V_f \tag{7}$$

$$\Delta V_c = \sqrt{\mu/R_c} - \sqrt{2\mu(1/R_a-1/R_c)/\left[(R_c/R_a)^2/\cos^2\gamma_f-1\right]} \tag{8}$$

Finally, the vehicle is in a circular orbit of radius R_c, moving with a velocity $V_c = \sqrt{\mu/R_c}$.

3. OPTIMAL TRAJECTORIES

For minimum-fuel maneuver, the objective is then to minimize the total characteristic velocity. A convenient performance index is the sum of the characteristic velocities for deorbit, boost, and reorbit. Thus,

$$J = \Delta V_d + \Delta V_b + \Delta V_c \tag{9}$$

Where, ΔV_d, ΔV_b, and ΔV_c are the deorbit, boost, and reorbit characteristic velocities respectively, and are obtained from (2) and (6) as

$$\Delta V_d = \sqrt{\mu/R_d} - (R_a/R_d)V_e\cos(-\gamma_e) \tag{10}$$

$$\Delta V_c = \sqrt{\mu/R_c} - (R_a/R_c)(V_f+\Delta V_b)\cos\gamma_f \qquad (11)$$

Alternatively, ΔV_d, ΔV_b and ΔV_c are also given by (3), (7), and (8) respectively. Let us note that for a given circular orbit of radius R_c, the impulses ΔV_b and ΔV_c are completely determined by the velocity V_f and the flight path angle γ_f at the exit. The velocity V_e and the flight path angle γ_e at the entry point are dependent only on the magnitude of the deorbit impulse ΔV_d. For a given atmospheric entry (i.e., for a given perigee altitude occurring within the atmosphere), we have a fixed value of ΔV_d and hence fixed values of entry velocity V_e, and entry flight path angle γ_e as seen from (1) and (2). The optimization problem is to minimize the total fuel consumption (i.e., maximizing the vehicle mass), for a given orbital inlination, and apogee altitude at LEO.

4. NUMERICAL DATA AND RESULTS

A typical AOTV configuration with high L/D is shown in Fig. 3. The liquid oxygen is stored in two separate tanks to provide a tapered nose, and inflated chins are used to continue this tapering along the body. A large deployable flap is provided to trim the vehicle at low angles of attack for maximum L/D performance. A representative set of numerical values used for a complete mission from GEO to SSO is given below[10].

weight of the vehicle = 112,625 N

aerodynamic reference area = 30.8 sq.m

aerodynamic reference length = 15.67m

gravitational constant of Earth = 3.96772×10^{14} m^3/sec^2

radius of Earth = 6356.766 km

altitude of atmospheric boundary = 120 km

altitude of GEO = 35884 km

altitude of SSO = 556 km

Prescribed conditions have the altitude of perigee in the atmosphere as 58 km, orbital inclination to be achieved during the amospheric maneuver as 25 degrees, and the altitude of space station orbit as 556 km. The control is achieved by bank angle modulation using a piecewise linear steering option of the POST. A constant angle of attack of 10 degrees corresponding to maximum lift-to-drag ratio of 1.724 and the 1976 US standard atmosphere, are utilized in the simulation.

Using the above mentioned data, the optimal solution has the following characteristic velocities:

Deorbit characteristic velocity, ΔV_d = 1491.04 m/sec

Boost characteristic velocity, ΔV_b = 24.58 m/sec

Reorbit characteristic velocity, ΔV_c = 156.36 m/sec

Total characteristic velocity ΔV = 1671.98 m/sec

The complete mission in terms of the velocity profile is shown in Fig. 4. Initially, the vehicle is in a circular orbit at GEO moving at a speed V_d = 3064.82 m/sec. A deorbit impulse ΔV_d = 1491.04 m/sec is executed to put the vehicle along the GEO-entry elliptic orbit. A specific impulse of 456 sec is used for all the characteristic velocities. The elliptic velocity at the deorbit point D is $\bar{V}_d = V_d - \Delta V_d$ = 1573.78 m/sec. At the atmospheric interface E of altitude H_a = 120 km, the vehicle attains an orbital velocity V_e = 10305.93 m/sec. During the atmospheric maneuver, the velocity of the vehicle

is depleted and the exit velocity is V_f = 7898.85 m/sec. In order to attain the desired SSO altitude H_c = 556 km, a boost impulse ΔV_b = 24.58 m/sec is required at the exit F from the atmosphere. Then the elliptic velocity at the exit is $\bar{V}_f = V_f + \Delta V_b$ = 7923.43 m/sec. The vehicle travels along the exit-SSO elliptic path and has a velocity $\bar{V}_c$ = 7419.74 m/sec at the reorbit point C. In order to insert the vehicle into a circular orbit at this altitude H_c = 556 km, a reorbit impulse ΔV_c = 156.36 m/sec is required. The vehicle is now in a circular path at SSO moving with a speed of $V_c = \bar{V}_c + \Delta V_c$ = 7576.1 m/sec. The vehicle takes 18,792 seconds for the GEO-entry portion, spends 470 seconds during the atmospheric maneuver, and finally requires 1,931 seconds for the exit-SSO portion. The total time taken for the complete mission is 5.8869 hours.

Fig. 5(a) gives the time history of altitude. The spacecraft enters and exits the atmosphere at an altitude of 120 km. The minimum altitude reached is 52.07 km. The velocity versus time is shown in Fig. 5(b). The vehicle enters the atmosphere with a velocity of 10305.93 m/sec and leaves the atmosphere with a speed of 7898.85 m/sec, thus giving a velocity reduction of 2407.08 m/sec. The profile of flight path angle with time is shown in Fig. 5(c). The spacecraft enters the atmosphere with an inclination of -5.169 degrees and exits with 1.8596 degrees. Fig. 5(d) depicts the orbital inclination of 25 degrees achieved during the atmospheric maneuver. Fig. 6(a) shows the variation of bank angle during the atmospheric flight. Fig. 6(b) gives the peak heating rate as 730 W/sq.cm. As shown in Fig. 6(c), the peak dynamic pressure is 30.33 KN/sq.m. According to Fig. 6(d), the maximum g-load is 4.69.

6. CONCLUDING REMARKS

In this paper, we have addressed the problem of minimization of fuel consumption during the atmospheric portion of an aeroassisted, orbital transfer vehicle with high L/D capability. The complete mission has required three characteristic velocities; a deorbit impulse at HEO, a boost impulse at the atmospheric exit, and a reorbit impulse at LEO. A performance index has been formulated as the sum of these three impulses. Fuel optimal trajectories have been obtained for the vehicle using POST. Future work is concerned with obtaining fuel-optimal trajectories with constraints on heating rate and acceleration.

ACKNOWLEDGEMENTS

This research work was supported by the grant NAG1-736 from Spacecraft Control Branch, NASA Langley Research Center, Hampton.

7 References

1. Walberg, G. D., "A survey of aeroassisted orbital transfer", J. Spacecraft, 22, 3-18, Jan.-Feb., 1985.

2. Vinh, N.-X., Optimal Trajectories in Atmospheric Flight, Elsevier Scientific Publishing Co., Amsterdam, 1981.

3. Dickmann, E. D., The effect of finite thrust and heating constraints on the synergetic plane change maneuver for space-shuttle orbiter-class vehicle, NASA TN D-7211, Oct. 1973.

4. Hull, D. G., Glitner, J. M., Speyer, J. L., and Maper, J., "Minimum energy loss guidance for aeroassisted orbital plane change", J. Guidance, Control, and Dynamics, 8, 487-493, July-Aug., 1985.

5. Vinh, N. X., and Hanson, J. M., "Optimal aeroassisted return from high Earth orbit with plane change", Acta Astronautica, 12, 11-25, 1985.

6. Miele, A., Baspur, V. K., and Lee, W. Y., "Optimal trajectories for aeroassisted noncoplanar orbital transfer", Acta Astronautica, 15, 399-412, June-July, 1987.

7. Mishne, D., and Speyer, J. L., "Optimal control of aeroassisted plane change maneuver using feedback expansions", Proc. AIAA Flight Mechanics Conf., Williamsburg, Aug., 1986.

8. Brauer, G. L., Cornick, D. E., and Stevenson, R., "Capabilities and Applications of the Program to Optimize Simulated Trajectories (POST)," NASA CR-2770, Feb. 1977.

9. Marec, J. P., Optimal Space Trajectories, Elsevier Scientific Publishing Company, Amsterdam, 1979.

10. Talay, T. D., White, N. H., and Naftel, J. C., "Impact of atmospheric uncertainties and viscous interaction effects on the performance of aeroassisted orbital transfer vehicles", AIAA 22nd Aerospace Science Meeting, Reno, NV, Jan. 9-12, 1984.

****

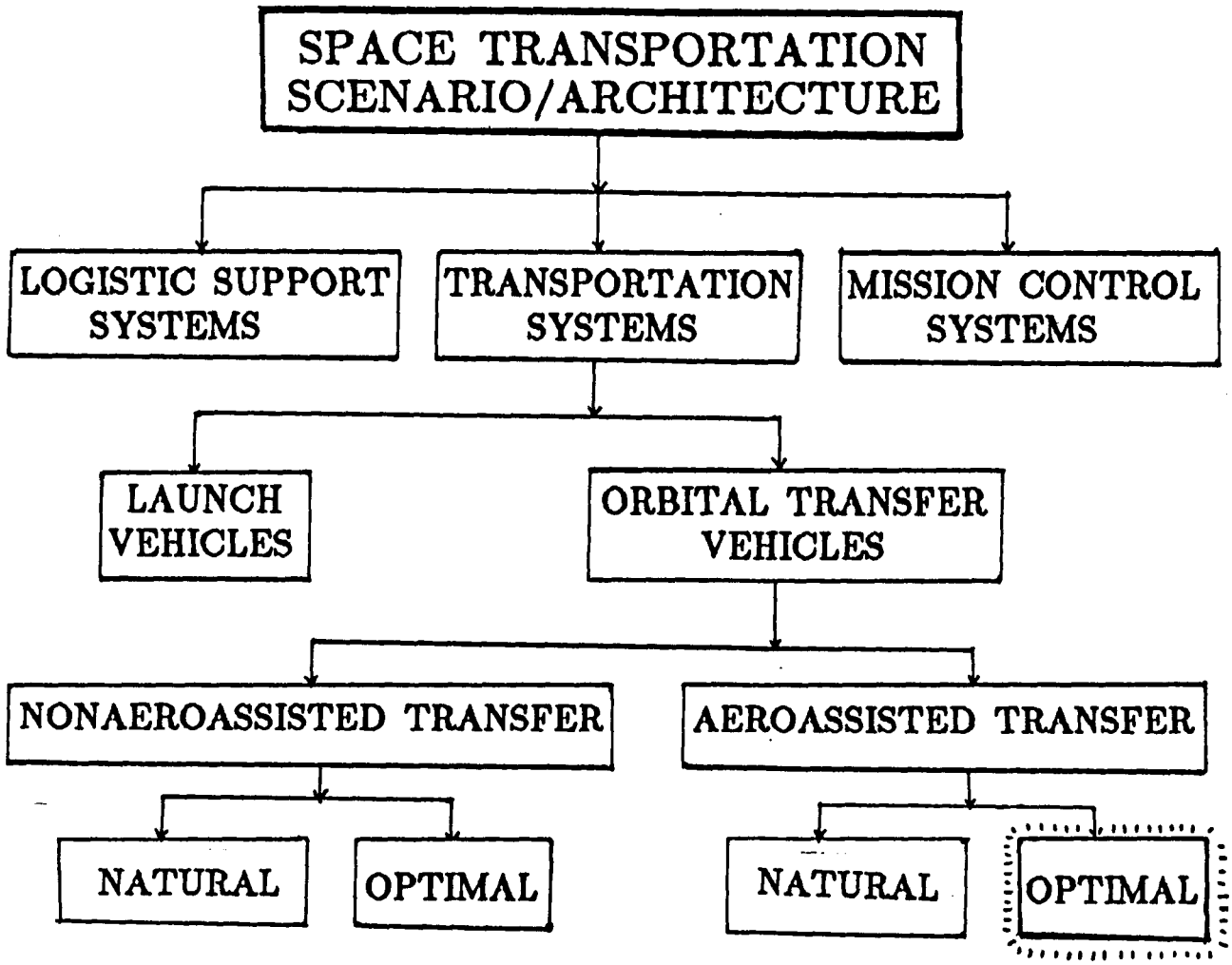

Fig.1 Space Transportation Architecture

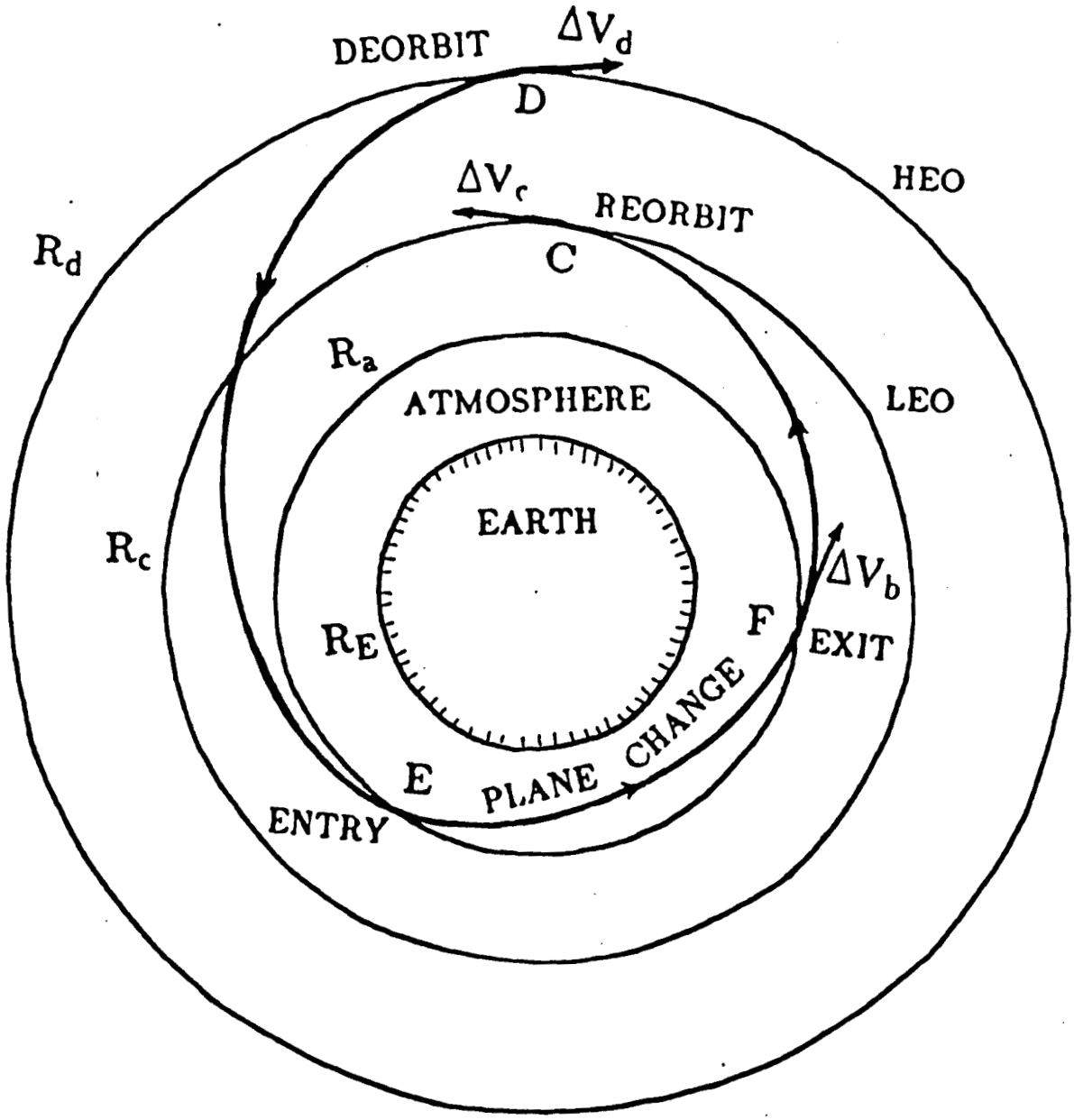

Fig. 2 Aeroassisted Orbital Plane Change

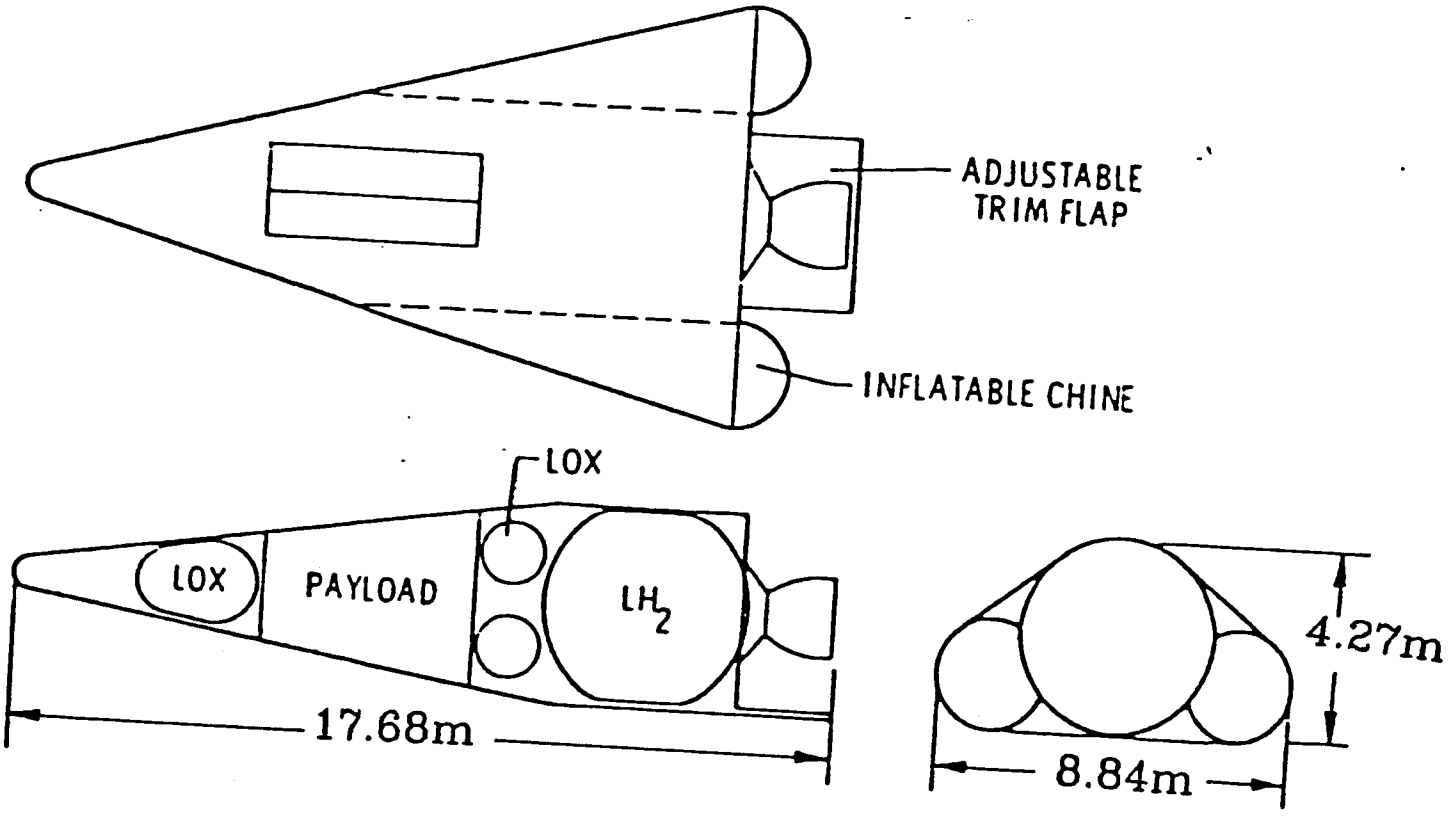

Fig.3 AOTV with high L/D capability

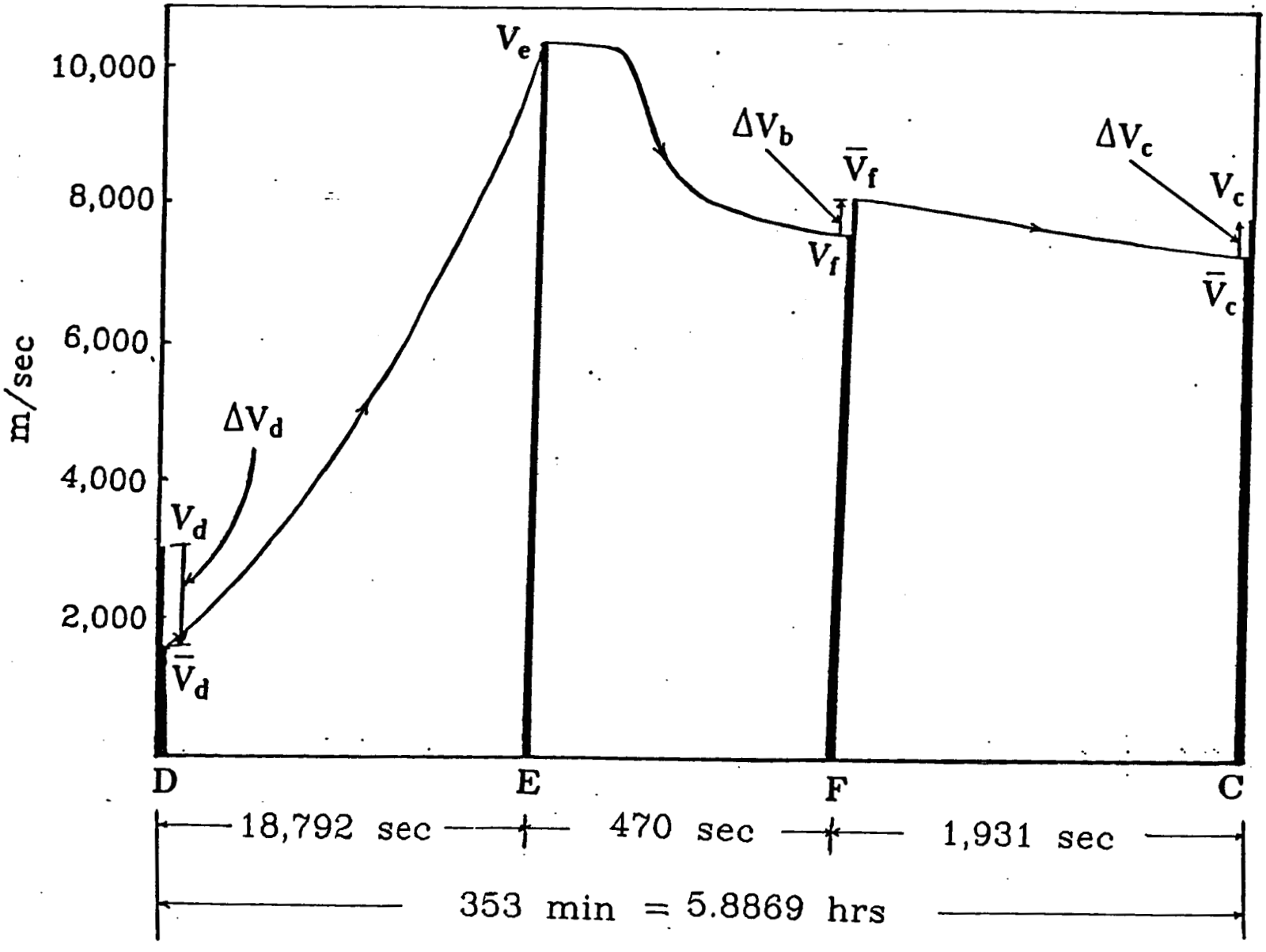

Fig.4 Velocity Diagram for the Complete Mission

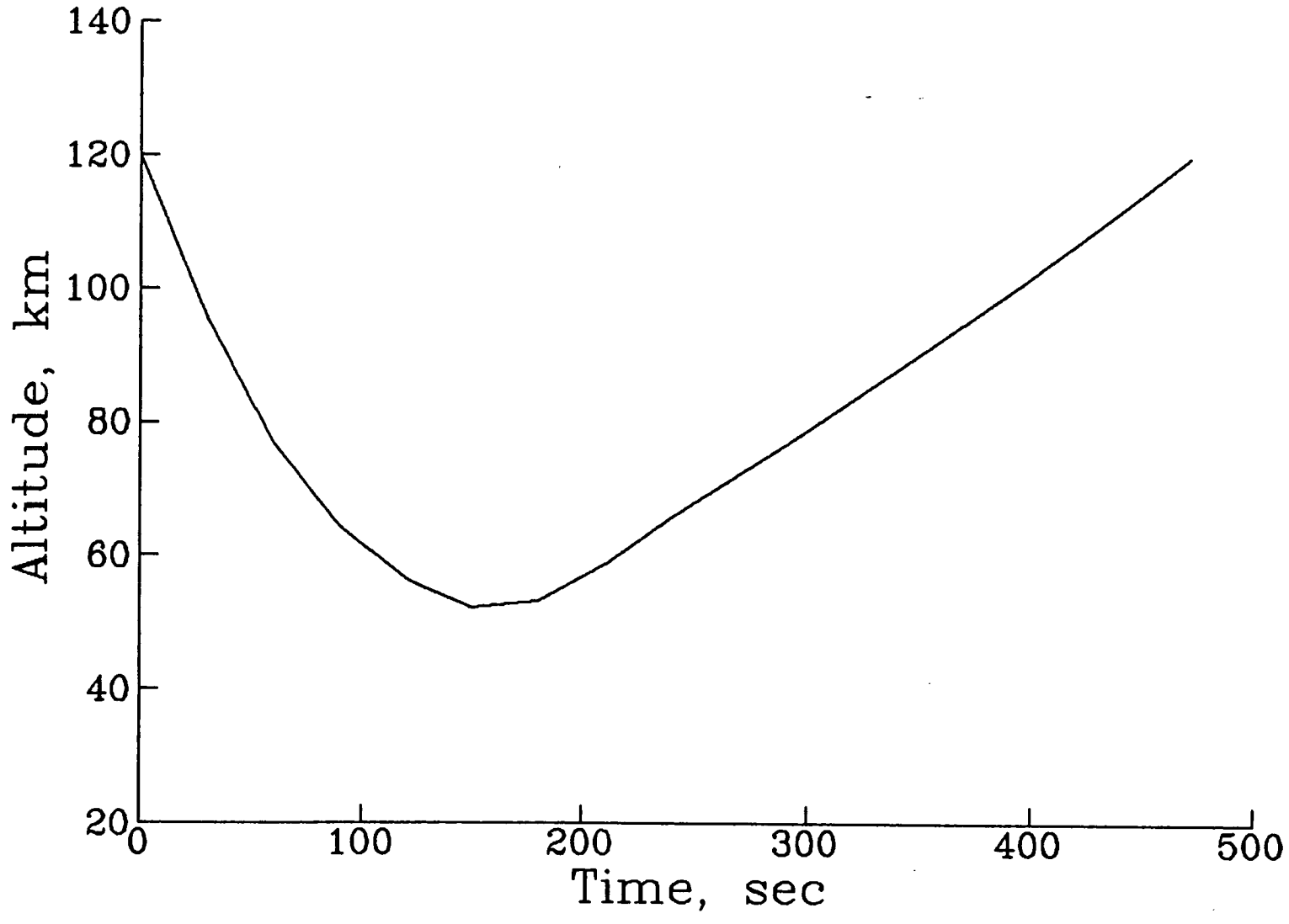

Fig.5(a) Time history of altitude

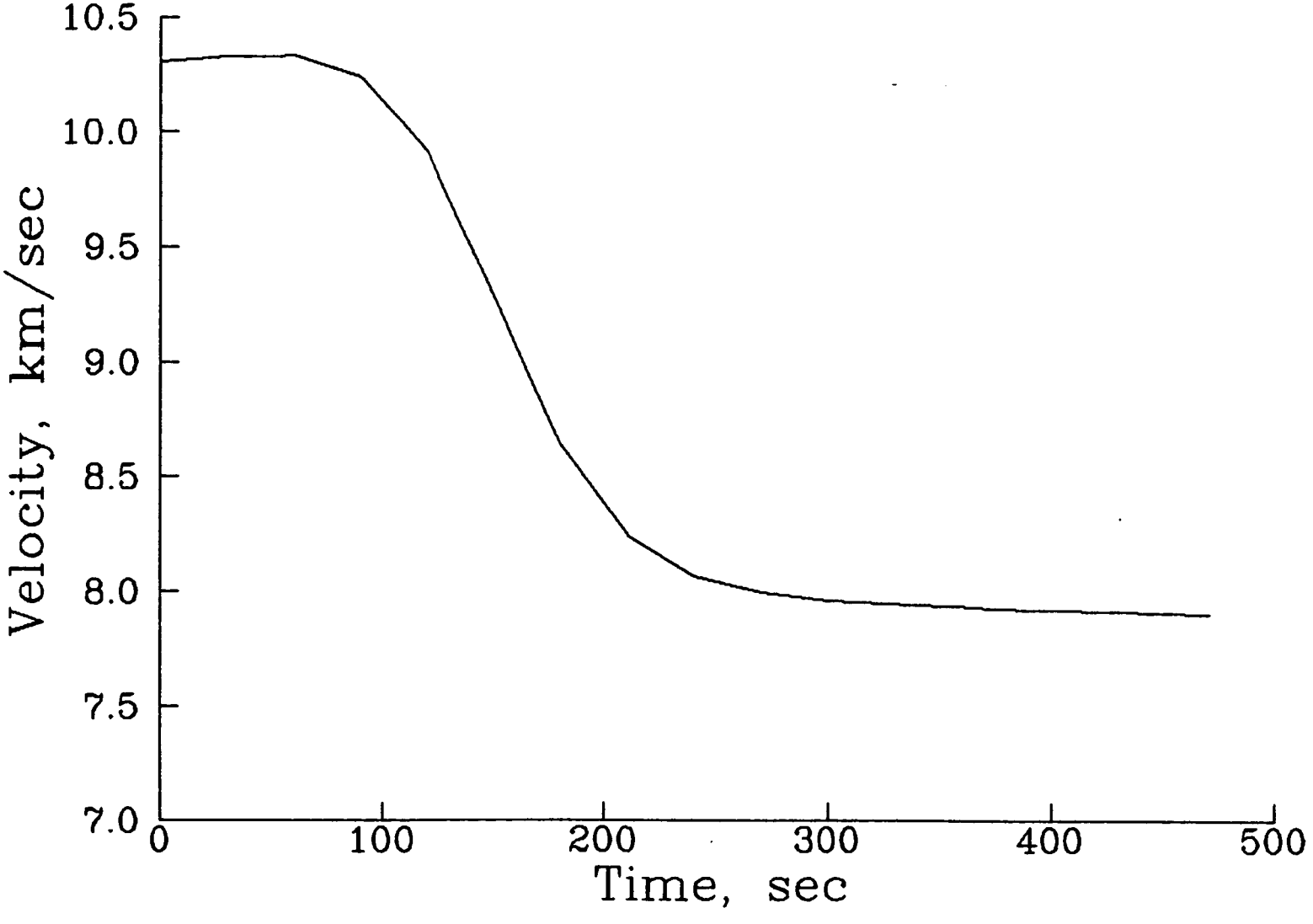

Fig.5(b) Time history of velocity

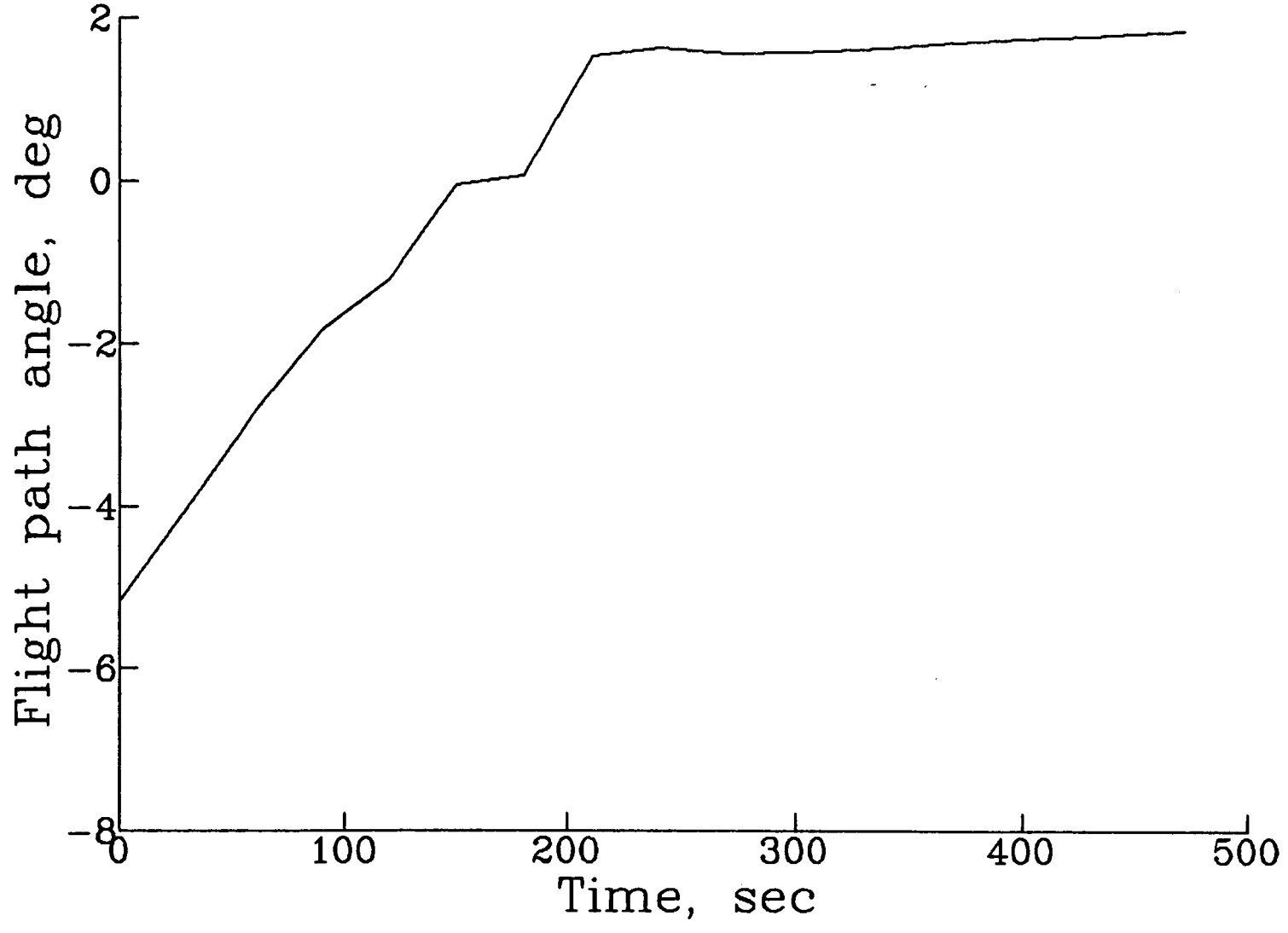

Fig.5(c) Time history of flight path angle

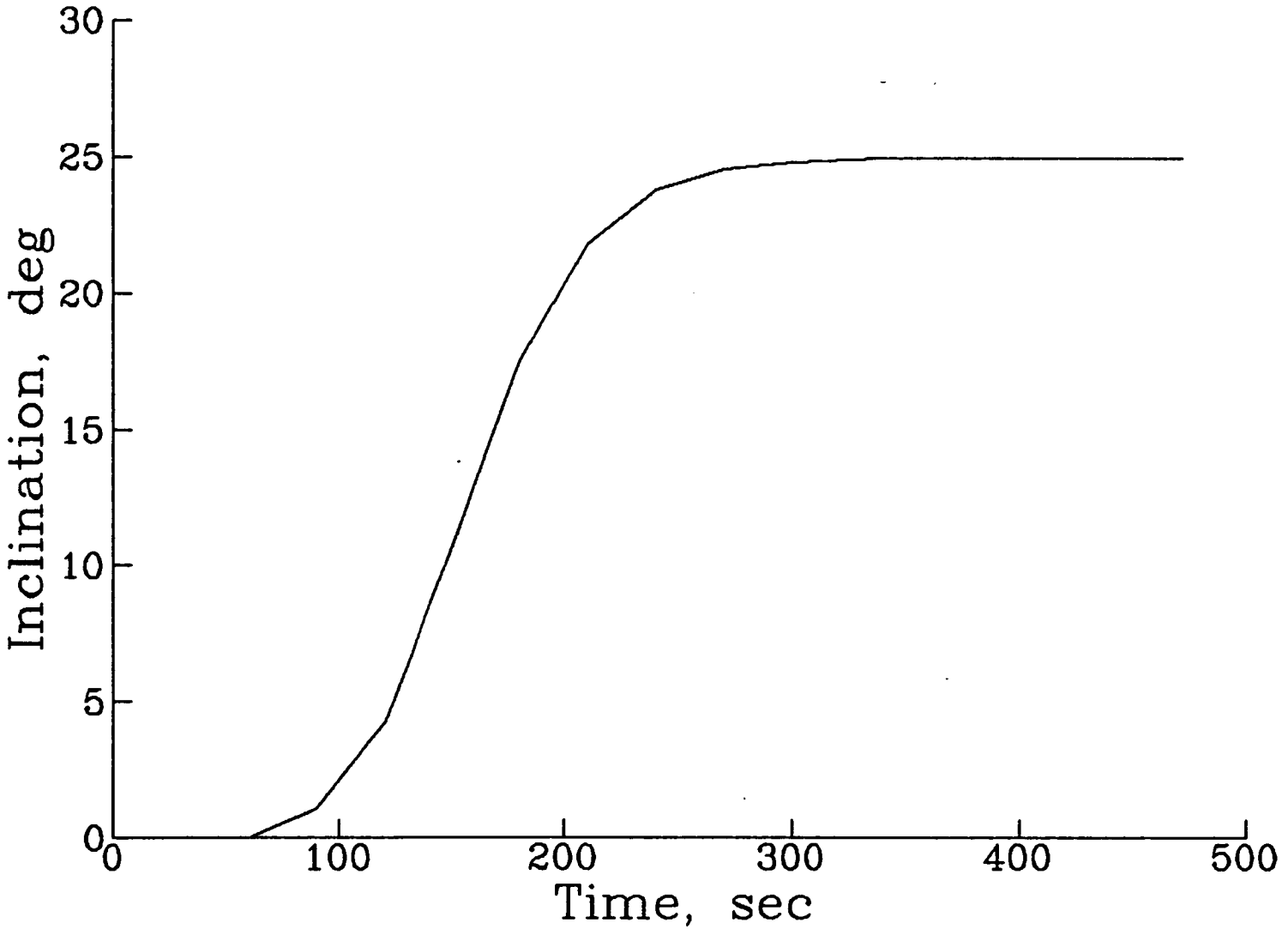

Fig.5(d) Time history of inclination

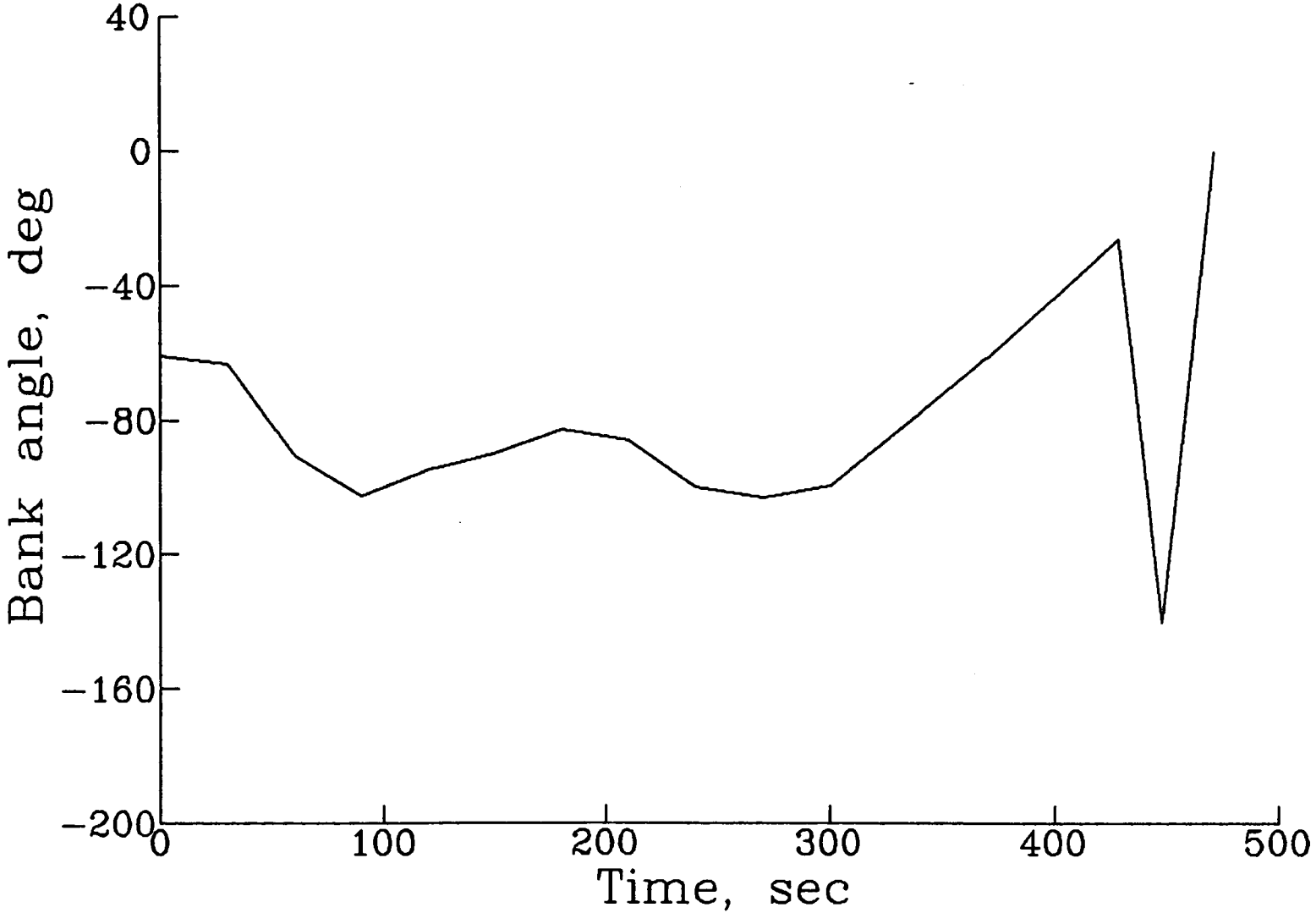

Fig.6(a) Time history of bank angle

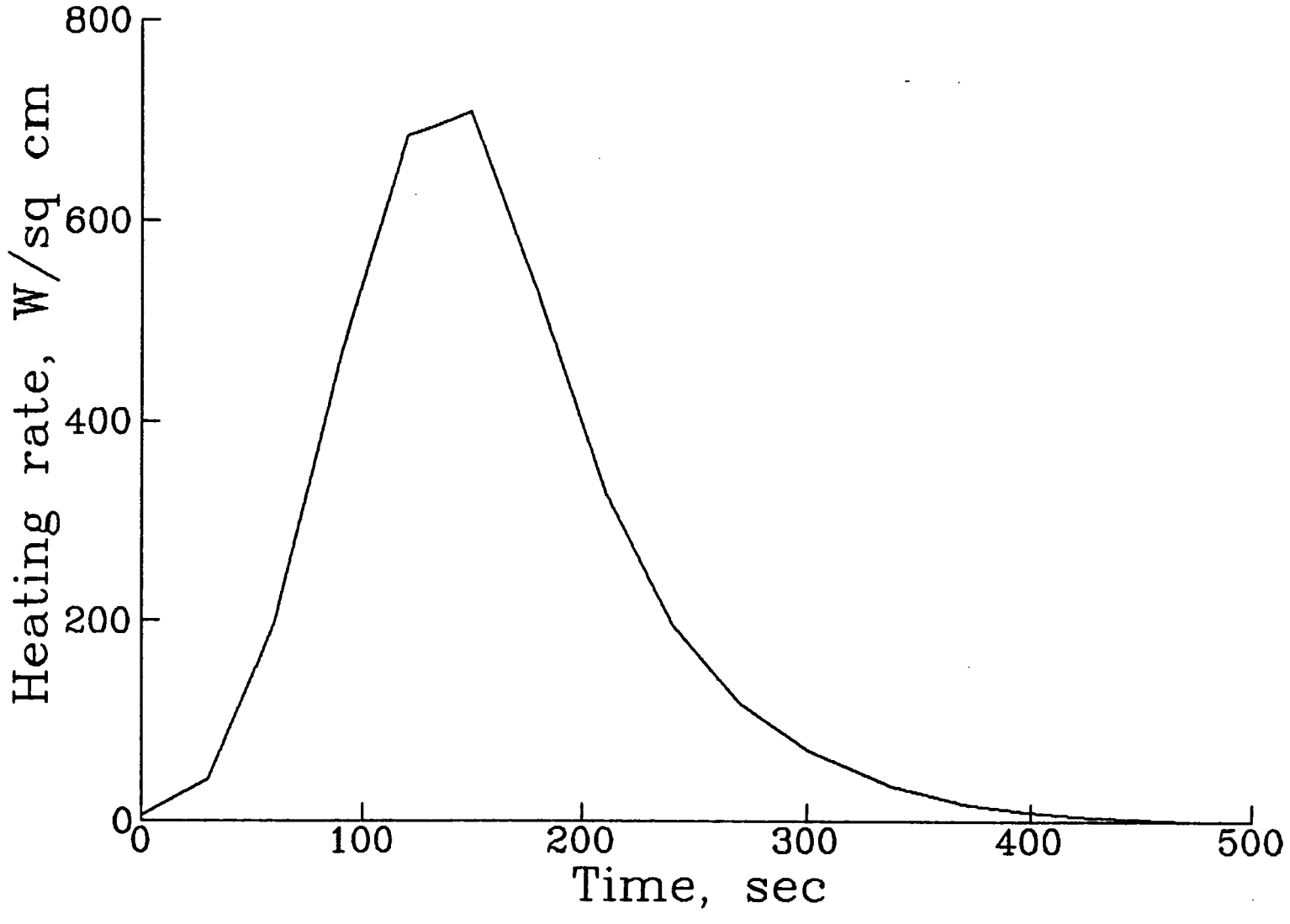

Fig.6(b) Time history of heating rate

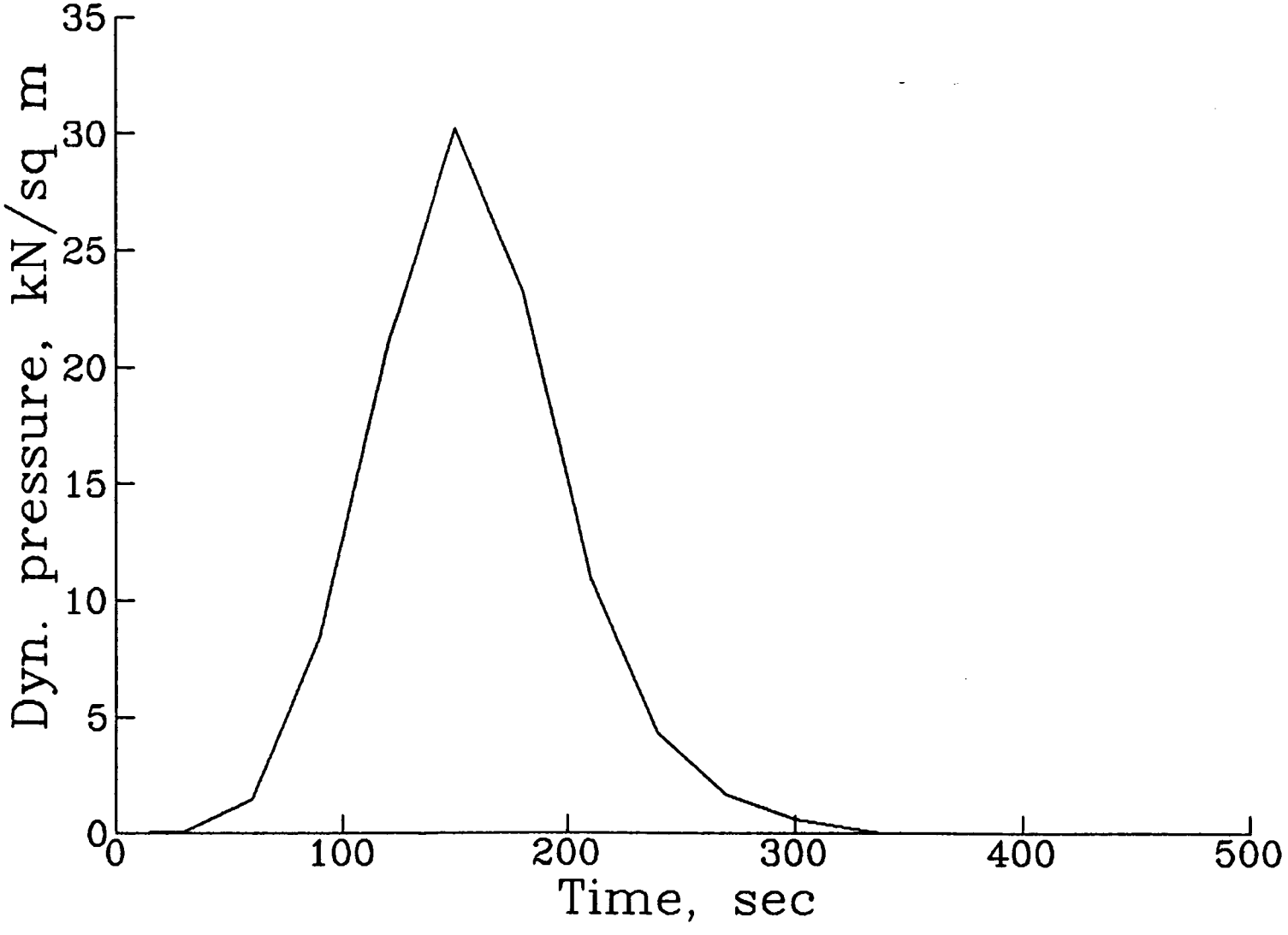

Fig.6(c) Time history of dynamic pressure

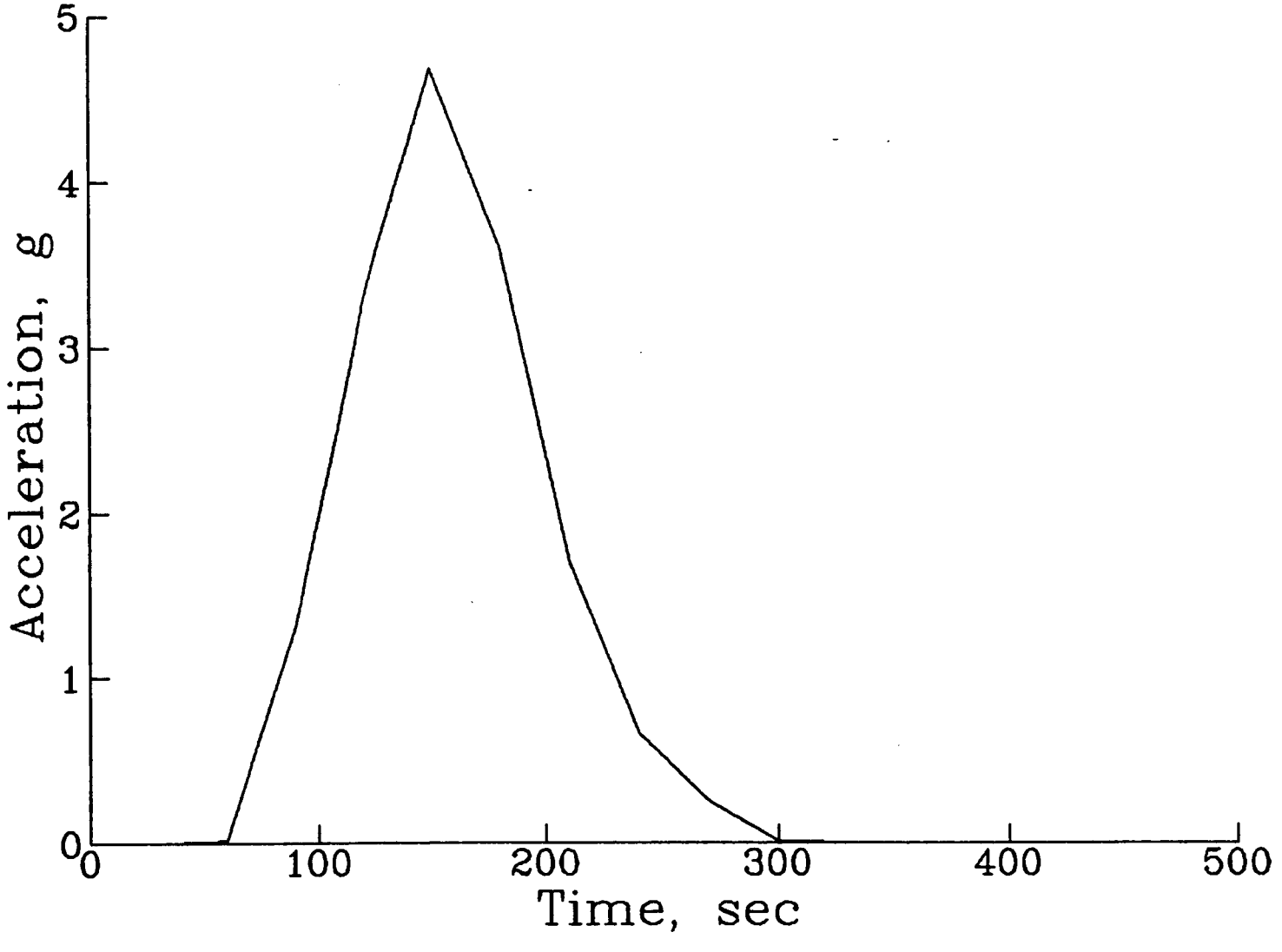

Fig.6(d) Time history of sensed acceleration